NOVA SCHOOL OF SCIENCE & TECHNOLOGY

DEPARTMENT OF PHYSICS

IGOR CAMPOS NECA

BSc in Biomedical Sciences

DEVELOPMENT OF A PORTABLE DEVICE FOR LOOP-MEDIATED ISOTHERMAL AMPLIFICATION TEST FOR DETECTION OF PATHOGENS

MASTER IN BIOMEDICAL ENGINEERING

NOVA University Lisbon
September, 2023

NOVA SCHOOL OF SCIENCE & TECHNOLOGY

DEPARTMENT OF PHYSICS

DEVELOPMENT OF A PORTABLE DEVICE FOR LOOP-MEDIATED ISOTHERMAL AMPLIFICATION TEST FOR DETECTION OF PATHOGENS

IGOR CAMPOS NECA

BSc in Biomedical Sciences

Adviser: Abel González Oliva
Associate Professor, ITQB

Co-adviser: Hugo Manuel Brito Águas
Associate Professor, FCT-NOVA

Examination Committee

Chair: Célia Maria Reis Henriques
Associate Professor, FCT-NOVA

Adviser: Abel González Oliva
Associate Researcher, ITQB

Member: Pedro Carlos de Barros Fernandes
Associate Professor, ULusofona

MASTER IN BIOMEDICAL ENGINEERING

NOVA University Lisbon
September, 2023

Development of a portable device for Loop-Mediated Isothermal Amplification test for detection of pathogens

This document was created with the (pdf/Xe/Lua)LaTeX processor and the NOVAthesis template (v6.10.17) [1].

Acknowledgements

I would like to express my heartfelt gratitude to the remarkable individuals who have played a pivotal role in my journey and the completion of this endeavor. Their unwavering support, love, and guidance have been instrumental in shaping my path to success.

First and foremost, I want to extend my deepest thanks to my beloved girlfriend, Rita. Your unwavering love, patience, and encouragement have been my anchor through the challenges of this endeavor. Your presence in my life is a constant source of inspiration, and I am profoundly grateful for your unwavering support.

To my mother, Maria, your endless sacrifices, boundless love, and unwavering belief in me have been the driving force behind my aspirations. All your actions have made me who I am, and for that I am grateful.

To my sister Ariana, that despite being in France, never forgot me. You always inspired me to do my best, and to have a brighter future. You are indeed the person I that inspired me to be my best self. Thank you.

My heartfelt gratitude also goes to my dear grandparents, Maria and Alfredo. Your stories, wisdom, and unwavering faith in me have been a source of motivation and comfort. Without your support, I would not be where I am now.

I would like to extend my appreciation to my academic adviser, Abel. Your guidance, mentorship, and belief in my potential have been instrumental in shaping my academic and professional journey. Your dedication to my growth as a scholar and individual has been invaluable. I am also indebted to the postdoctoral researcher in our lab, Dragana. Your presence in the lab made me calm in the most desperate times.

I would like to acknowledge the support of all family who have stood by me throughout this journey. Your encouragement and understanding have meant the world to me.

Lastly, I would like to thank to my closest group of friends. Altough we now are apart from each other, we all have a strong bound, where we have uncoditional support from each other. Thank you IDP!

To each of you, I extend my heartfelt thanks. This achievement would not have been possible without your unwavering support and belief in me. I am truly fortunate to have such incredible people in my life.

”

“The difference between a novice and a master is that a master has failed more times than a novice had tried.”

— Anonymous

Abstract

Fecal contamination of soil and water in beaches and other recreational areas has been a persistent problem. Every year, approximately 120 million cases of gastrointestinal diseases and 50 million cases of severe respiratory infections caused by swimming and bathing in fecally polluted coastal waters are reported, directly impacting public health. Nowadays, there are several approaches to detect these pathogens, such as Polymerase Chain Reaction (PCR) and culture-based methods. However, most of these methods have long turnaround times between sample collection and obtaining results, and they often require a laboratory environment for execution.

The Loop mediated isothermal amplification (LAMP) method stands out due to its remarkable sensitivity and specificity, enabling the detection of minute quantities of bacteria within a given sample. The objective of this study was to design and construct a portable device that could be used outside the laboratory.

Simulations were carried out to ascertain the optimal approach for constructing the heating chamber, while additional simulation software was employed to enhance our comprehension of the electrical components necessary for building the circuit. A detailed inventory of these components is provided, along with the code developed for the microcontroller. Additionally, studies were conducted to assess power consumption, heating time, and temperature sensor calibration. A housing box for all the components was custom-designed using 3D printing technology.

The LAMP assays were successful, validating the results of the aforementioned experiments. The code effectively enabled the microcontroller to read data from both temperature sensors, allowing for the adjustment of power delivered to the heating element. Furthermore, it accurately displayed relevant information on the heating chamber's screen. Additionally, the code provided users with the ability to customize the assay duration, initiate and pause it, and appropriately illuminate LEDs to reflect the assay's status.

The research work described in this dissertation was carried out in accordance with the norms established in the ethics code of Universidade Nova de Lisboa. The work described and the material presented in this dissertation, with the exceptions clearly indicated,

constitute original work carried out by the author Igor Campos Neca.

Keywords : LAMP assay, DNA amplification, Portable device, Simulation, Instrumentation

Resumo

A contaminação fecal do solo e da água em praias e outras áreas de lazer tem sido um problema persistente. Todos os anos, são relatados aproximadamente 120 milhões de casos de doenças gastrointestinais e 50 milhões de casos de infecções respiratórias graves causadas por nadar e banhar em águas costeiras poluídas por fezes, o que impacta diretamente na saúde pública. Atualmente, existem várias abordagens para detectar esses patógenos, como a Polymerase Chain Reaction (PCR) e métodos baseados em cultura. No entanto, a maioria desses métodos apresenta longos tempos de espera entre a coleta da amostra e a obtenção dos resultados, além de exigirem frequentemente um ambiente de laboratório para a execução.

O método de Loop mediated isothermal amplification (LAMP) é destacado devido à sua notável sensibilidade e especificidade, permitindo a detecção de quantidades mínimas de bactérias dentro de uma amostra dada. O objetivo deste estudo foi projetar e construir um dispositivo portátil que pudesse ser usado fora do laboratório.

Foram realizadas simulações para determinar a abordagem ótima para construir a câmara de aquecimento, enquanto outro software de simulação adicional foi utilizado para aprimorar a compreensão dos componentes elétricos necessários para montar o circuito. Um inventário detalhado desses componentes é fornecido, juntamente com o código desenvolvido para o microcontrolador. Além disso, foram conduzidos estudos para avaliar o consumo de energia, o tempo de aquecimento e a calibração do sensor de temperatura. Uma caixa de alojamento para todos os componentes foi projetada utilizando a tecnologia de impressão 3D.

Os ensaios LAMP foram bem-sucedidos, validando os resultados dos testes mencionados anteriormente. O código permitiu efetivamente que o microcontrolador lesse dados de ambos os sensores de temperatura, permitindo o ajuste da potência entregue ao elemento de aquecimento. Além disso, exibiu com precisão informações relevantes na tela sobre a câmara de aquecimento. O código ofereceu aos usuários a capacidade de personalizar a duração do ensaio, iniciá-lo e pausá-lo, e ativar adequadamente LEDs para refletir o status do ensaio.

O trabalho de investigação descrito nesta dissertação foi realizado de acordo com as

normas estabelecidas no código de ética da Universidade Nova de Lisboa. O trabalho descrito e o material apresentado nesta dissertação, com as exceções claramente indicadas, constituem trabalho original realizado pelo autor Igor Campos Neca.

Palavras-chave : Teste LAMP, Amplificação de DNA, Dispositivo portátil, Simulação, Instrumentação

Contents

List of Figures

List of Tables

Abbreviations

ASA	Acrylonitrile Styrene Acrylate
B3	Backwards 3
BIP	Backward Inner Primer
BJT	Bipolar junction transistor
CAD	Computer-aided design
cfu	colony forming units
DNA	Deoxyribonucleic acid
F3	Forward 3
FEA	Finite element analysis
FIP	Forward Inner Primer
IDE	Integrated development environment
LAMP	Loop mediated isothermal amplification
LCD	Liquid crystal display
LED	Light emitting diode
MOSFET	Metal–oxide–semiconductor field-effect transistor
NTC	Negative Temperature Coefficient
OLED	Organic light-emitting diode
PA-LAMP	Primer-activatable loop-mediated isothermal amplification
PCR	Polymerase Chain Reaction

PETG	Polyethylene terephthalate glycol
PLA	Polylactic acid
POC	Portable point-of-care
pwm	Pulse width modulation
RDT	Rapid Diagnostic Test
RGB	red, green and blue
RNA	Ribonucleic acid
RT-PCR	Reverse Transcriptase Polymerase Chain Reaction
SARS-CoV-2	Severe acute respiratory syndrome coronavirus 2

1 Introduction

Fecal contamination of soil and water of beaches and other recreational waters has been a problem, since yearly, around 120 million cases of gastrointestinal disease and 50 million of severe respiratory infection caused by swimming and bathing in fecal polluted coastal waters are reported, thus having a direct impact on health. Although an improvement of water quality in recreational waters can be observed, the need of monitoring fecal contamination still exists since it is a harm to human health. The most common method of monitoring it is by detecting *Escherichia coli* and *Enterococcus faecalis*, as they are frequently present in the intestines of humans and animals. Their presence indicates potential fecal contamination [2].

Nowadays, there are several approaches to detect these pathogens, such as Polymerase Chain Reaction (PCR) [3], culture-based methods, or microscopy [4–6]. Unfortunately, many of these methods exhibit significant delays between sample collection and obtaining the final results, along with a high level of specificity and low sensitivity. It can occasionally lead to false negatives, and these methods are typically limited to laboratory environments. In more recent years, there has been a growing significance attributed to a novel technique known as the Loop mediated isothermal amplification (LAMP) method. This method exhibits a remarkable level of sensitivity and specificity, enabling the detection of minute quantities of bacteria within a given sample. Moreover, the LAMP method boasts a rapid processing time, obviating the need for thermal cycling. Additionally, this technique has the capability to identify multiple targets simultaneously within a single reaction [7].

The objective of this study was to design and construct a portable device with the ability to carry out LAMP. The device's capacity to conduct rapid and precise tests on-site has the potential to effectively detect potential health hazards, thereby significantly reducing the transmission of illnesses in locations where pathogens are present. Additionally, this technology can minimize the duration of site closures and mitigate the occurrence of false negative results. Furthermore, it was required to develop a filtration system that was capable of effectively concentrating pathogens while simultaneously removing undesirable components. One notable advantage in comparison to conventional methods is the cost-effectiveness of the LAMP assay, rendering it accessible to developing nations

and facilitating regular testing without excessive expenditure of time and resources.

In order to facilitate LAMP assays, it was necessary for the device to possess thermostabilized heating chambers that can accommodate 0.5 mL eppendorf reaction tubes. These tubes serve as the site for the reaction, housing both the sample and the necessary components. Additionally, the device must be equipped with a heating element capable of effectively increasing the temperature. To ensure precise control over the temperature, electronic circuitry was required to maintain the desired level. Furthermore, a timer was essential to accurately monitor the duration of the assays as well as Light emitting diode (LED) indicators and switches.

To achieve the long-term outcome, the device had to undergo a design process employing drawing and simulation software. This allowed for a comprehensive preview of the required circuitry and the thermal capabilities of the materials, as well as the necessary heating elements. Subsequently, a prototype was constructed, followed by laboratory validation.

1.1 State of the art

1.1.1 Methods to detect pathogens

In 1677 Antonie van Leeuwenhoek was the first to use microscopy to describe spermatozoa, thereby standardizing the technique. It is typically used to observe larger hazards, such as parasites. Due to the assay's low sensitivity, the required time and reliance on expert personnel can result in the illness of multiple individuals [3–5, 8].

Used in 1876 by Robert Koch and refined in 1950, culture was the next gold standard. Culture refers to a process of growing microorganisms, (*e.g. E.coli*), in controlled environments with nutrients and environment conditions (*e.g.* temperature, pH) that are optimal to the microorganism meant to grow. The assessment of pathogen resistance to antibiotics through cultural analysis allows for the identification of the most appropriate treatment for the patient, while also providing researchers with a comprehensive understanding of the situation. Regrettably, certain specimens pose challenges in terms of cultivation due to their inherent difficulty and exceptionally sluggish growth rates. Additional drawbacks include the requirement for operator expertise and the considerable time investment [4, 9].

Currently, various detection methods are available, with some frequently employed ones outlined in table 1.1. Among these methods, Ian R. Poxton indicates that nucleic acid amplification techniques such as PCR and LAMP are considered to be the most sensitive and specific [4].

Table 1.1: Sensitivity and specificity of *Chlamydia trachomatis* testing [4]

Method	Sensitivity, %	Specificity , %
Culture	70-90	100
Nucleic acid amplification	90-100	97-100
DNA probe	67-96	96-100
Immunofluorescence	70-100	> 95
Enzyme immunoassay	43-92	92-100

The Loop mediated isothermal amplification , is a molecular diagnostic method that amplifies a specific DNA or RNA sequence within a sample using a set of primers and a DNA polymerase enzyme. The method was first developed in 2000 by T. Notomi *et al*. [7].

Its ability to amplify DNA or RNA at a constant temperature, high specificity, and sensitivity make it a useful tool for the diagnosis of infectious diseases and genetic disorders. Its simple instrumentation and low cost make it an accessible and portable alternative regarding PCR, particularly in resource-limited settings.

The principle of a LAMP test is based on the isothermal amplification of a specific target, DNA or RNA sequence, using a set of primers that bind to the target sequence. The primers are designed to bind to specific regions of the target sequence, known as the loop and the stem regions. The DNA polymerase enzyme then uses the primers as a template to synthesize new copies of the target sequence, which results in the exponential amplification of the target sequence.

The basic test procedure can be divided in steps [10]:

1. When the temperature reaches 65 degrees Celsius (°C) and DNA polymerase with strand displacement activity is introduced, it becomes feasible to separate a double-stranded DNA molecule into two single-stranded molecules.

2. The Forward Inner Primer (FIP) (which has the first region complementary with the third region of itself, and not with the target DNA sequence) can now attach to the strand in 3', and with DNA polymerase, it synthetases a complementary one.

3. Since the initial region is not bonded to anything, another primer Forward 3 (F3) can anneal to it and initiate a new synthesis, thereby releasing the FIP.

4. Repeat the steps 2 and 4, but instead of starting the synthesis in 3', it will be done in 5', with Backward Inner Primer (BIP) and primer Backwards 3 (B3).

5. As mentioned in step 3, the first and third regions of either 3' or 5' are complementary, compelling them to bind, which should result in a DNA strand shaped like a dumbbell. Figure 1.1 depicts a schematic representation of the process undertaken until the current stage.

6. After having this DNA structure, the amplification process will take place by simply adding BIP and FIP to the solution. For enhanced visual representation, a video can be accessed on the website of the creators [11].

One of the key advantages of the LAMP test is the ability to perform cycles at a constant temperature, typically around 60-65°C, rather than the cycling temperature required for PCR. This simplifies the instrumentation and increases the accessibility of the test, making it suitable for use in resource-limited settings. Additionally, the LAMP test can be performed using a heating device, such as a laboratory water bath, making it a portable and low-cost alternative to PCR.

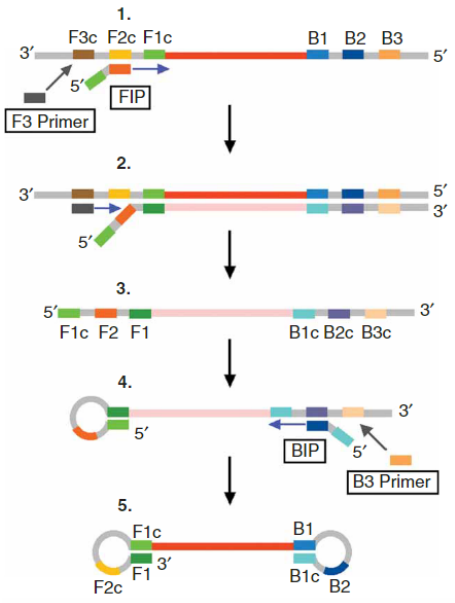

Figure 1.1: Obtaining the DNA structure to amplification adapted from [12]

Furthermore, the test can also be used to detect very specific mutations in genes, since the primers have to be built for only a specific sequence. Wen Fang Du *et al.* (2019) proved that it is possible to detect a single nucleotide with a type of LAMP called the Primer-activatable loop-mediated isothermal amplification (PA-LAMP)[13].

Since the initial publication of the LAMP assay, scientists have conducted numerous investigations to evaluate its performance, primarily driven by its notable benefits, including cost-effectiveness and precision. To date, several nations have embraced this assay as their definitive benchmark for pathogen identification. In the event that the primers are inadequately designed, the assay's specificity is compromised, as amplification solely develops when all gene regions that bind to the primers in a specific sequence are present. Consequently, the assay has the potential to yield inaccurate outcomes due to the amplification of an incorrect gene [14]. One notable advantage in comparison to PCR is its reduced susceptibility to inhibitory substances, resulting in an easier processing and DNA extraction process [15, 16].

Meanwhile, there is already an establish number of points that are used to optimize the LAMP assay, such as:

1. According to Notomi T. (2002), the addition of two other primers to the loop in the LAMP structure can cut the assay time in half (*e.g.* 30 minutes instead of an hour) [17].

2. As the molecule magnesium pyrophosphate can induce turbidity, it is possible to analyse the sample's turbidity instead of fluorescence after the assay. This insoluble molecule is generated during DNA synthesis. [18].

3. Because the magnesium ions are bind to the pyrophosphate ones, some bright fluorescence can be observed by adding calcein [12].

The process of primer selection can be perceived as a drawback due to its inherent complexity. However, there is already existing software available that automates the selection process, relieving researchers from the burden of manually going through it [19].

LAMP was mainly used to detect pathogens that commonly appear in food (foodborne diseases), such as *Salmonella* and *Escherichia coli* [14], [20]. All of these tests have successfully demonstrated that the specificity and sensitivity are equivalent to those of PCR when the appropriate set of primers is utilized for amplification. Given the complexity and time-intensive nature of optimizing primers for assay performance, successful primers could potentially be marketed and sold as part of commercially available kits.

The LAMP technique can serve as a viable substitute for PCR assays in detecting pathogens that have a direct impact on human health, including *Candida*, *Streptococcus pneumoniae*, Zika virus, and others. The distinguishing factors between each assay may lie in the extraction method employed and the specific primers utilized [16, 21, 22].

As an illustration, Candida is an opportunistic fungus that can impact various parts of the body such as the skin, vagina, bronchial lungs, and even prosthetic devices. It is worth noting that there is a growing prevalence of Candida strains that exhibit resistance to Azole compounds, which are commonly employed for the prevention and treatment of candidiasis [23]. Among the various methods currently available (such as CHROMagar, Germ tube production, and PCR), the LAMP technique stands out as the most favorable option. This is primarily due to its simplicity, rapidity, cost-effectiveness, sensitivity, and absence of the limitations associated with PCR, such as the requirement for expensive thermocyclers and gel documentation. In addition, conclusions can be drawn regarding the expeditious outcomes, ease of implementation, and high level of responsiveness exhibited by this approach. Consequently, it is well-suited for use in both laboratory and field settings. The samples may encompass a variety of bodily fluids, including vaginal secretions, urine, blood, sputum, synovial fluid, and bronchoalveolar lavage fluid. The researchers utilized DNA extraction kits to acquire the desired genetic material [21].

Another example can be observed in a clinical environment where the identification of the influenza virus takes place. This virus can be detected with other commercially

Rapid Diagnostic Test (RDT)s or Reverse Transcriptase Polymerase Chain Reaction (RT-PCR). Once more, after the proper optimization, the LAMP showed better sensitivity and specificity then RDTs [24], and RT-PCR [25], as well as the same detection limit.

One of the most recent applications of the LAMP assay, was in the detection of Severe acute respiratory syndrome coronavirus 2 (SARS-CoV-2) in clinical samples. Amaral *et al*. (2021) describe the possibility of obtaining a binary response (yes or no) via a colorimetric change made feasible by the detection of DNA polymerase reaction by-products [26]. In order for a Portable point-of-care (POC) test to be cost-effective, it must be constructed with minimal amounts of materials and reagents. Amaral *et al*. (2021) also refer the significance of knowing the samples we are working with, as the colorimetric assay is typically based on the pH change principle.

Since Amaral *et al*. (2021) were using saliva, a substance that changes pH from each person, they developed a new method where after the assay a mixture of zinc and murexide (Zn-MX) was added to the solution, changing the color from yellow to pink. The principle of the reaction is that the by-product pyrophosphate reacts with zinc, removing them from the compound Zn-MX, changing the color of MX [26].

In the present study, it was noted that the pH levels of the samples may exhibit variability. Consequently, the most suitable approach employed will be the aforementioned final method.

1.1.2 Portable devices for Point of care testing

By enabling quick and easy access to diagnostic data, portable POC testing equipment is essential to modern healthcare. These tools make it possible for medical practitioners to carry out diagnostic procedures on patients at the facility where they are being treated, saving time and money by eliminating the need for patients to travel to a centralized laboratory. Compared to traditional laboratory testing, portable devices also have a number of advantages, such as quicker turnaround times for test results, better patient outcomes and lower healthcare costs. Making assays portable also enables healthcare providers to conduct tests in rural or resource-constrained locations where laboratory facilities might not be easily accessible.

Technological developments like microfluidics, biosensors, and nanotechnology have made it possible to create small, inexpensive, and simple-to-use portable devices for Portable point-of-care (POC) testing and to miniaturize assays [27, 28]. As a result, this type of testing has grown in relevance in contemporary healthcare and is anticipated to do so going forward.

Before actually constructing the portable device,simulations of software towards heating capabilities can be created since:

1. Simulation allows designers and engineers to test the safety of a portable heating device before it is manufactured. This can help identify and address potential hazards or safety concerns before they become a problem in real-world use.

2. It can help optimize the performance of a portable heating device, such as its heating efficiency or energy consumption by simulating different design variations and operating conditions.

3. Has the potential to mitigate the expenses and time constraints linked to the process of reengineering and reevaluating a device subsequent to its production.

4. Assists in guaranteeing the optimal and effective performance of the device across a diverse array of real-life situations.

5. The utilization of simulation technology can contribute to the advancement of environmentally conscious and sustainable devices by minimizing resource consumption. This is achieved through a reduction in the number of physical prototypes required for testing purposes.

Using an Arduino microcontroller offers several advantages for building a portable prototype device. Arduino microcontrollers are relatively inexpensive, making them a cost-effective choice. They come with a user-friendly Integrated development environment (IDE) that includes a multitude of libraries, allowing for quick prototyping and testing. It is compatible with a wide range of sensors available in the market, providing flexibility in sensor selection. Additionally, Arduino is open source, permitting users to freely use or modify both software and hardware components. Furthermore, the microcontroller community is vast and active, making it a valuable resource for project assistance and guidance throughout the development process.

There exist a limited number of literary references pertaining to devices utilizing Arduino technology for the execution of LAMP or PCR assays in non-laboratory settings [27, 29–31]..

Sheu, Song, and Chen (2022) devised a portable system for PCR testing in which a pump is used to transfer the sample via a microfluidic route in order to execute the cycling in zones with a predefined temperature supplied by a cartridge heater [27]. This prototype's microfluidic path building requires several components and precise effort. Moreover, trained workers are required to operate the gadget. Velders, Schoen, and Saggiomo (2018) proposed an approach very similar to the one that was explored in this work [29]. The article exclusively focuses on the construction of Arduino shields. Due to the absence of contamination protection on the equipment, the customer lacks assurance regarding the device's ability to operate effectively across various environments.

Papadakis *et al*. (2022) developed a portable real-time colorimetric LAMP method, which offers a quantitative analysis approach, on which they aimed to make all the assay in one single reaction tube, preventing contaminations. This phenomenon occurs as a result of the dependence on the identification of varying shades of color in phenol-red. Additionally, the device was constructed using Computer-aided design (CAD) software, and its components were subsequently manufactured in 3D printing. A smartphone

application was developed to display the results in real time. In order to accomplish the aforementioned objectives, it is not feasible to solely rely on an Arduino for performing the necessary programming tasks to monitor changes in red, green and blue (RGB) pixel values. This limitation arises due to the inherent challenges associated with image manipulation on a microcontroller platform. In order to accomplish this, a more intricate machine, namely the Raspberry Pi, was chosen. Given our objective of adopting a binary approach, it is unnecessary to incorporate intricate components, therefore improving the affordability of the device. Moreover, the projected duration for the operation of this device utilizing a power supply with a capacity of 10000 mAh is approximately 5 hours [32]. Our objective is to achieve a similar or superior result while being able to prioritize a cost-effective setting, allowing for independent operation without the need for a phone.

Furthermore, Papadakis *et al*. (2022) employed a pH alteration technique as their chosen method of detection. In certain instances, such as in the case of saliva, there is a possibility of variation in pH levels from the test sample, which has the potential to introduce bias into the outcomes [26, 32]. Papadakis *et al*. (2022) further substantiates the feasibility of employing LAMP assays for the detection of diverse pathogens in unprocessed human body samples such as saliva, tissue, and swabs. Although our research focuses on the detection of pathogens in recreational waters, the aforementioned examples provide evidence that our device could be readily applied to other detection scenarios. The key distinctions lie in the methods employed for sample collection and treatment, as well as the specific primers utilized for the amplification process. In the present study, the treatment procedure involved the filtration of seawater followed by exposure to a LAMP mixture. The primers exhibit specificity towards individual pathogens.

Velders, Schoen, and Saggiomo (2018) study several observations regarding the device's distinctiveness. They proposed modifications aimed at reducing manufacturing costs and simplifying the production process, thereby eliminating the need for extensive expertise in electronic engineering. Additionally, they emphasized the device's user-friendly nature, ensuring accessibility to individuals of all skill levels. These enhancements were achieved through the utilization of electronics and open-source software [29].

In this thesis, the subsequent procedures had been taken into account [29, 33]:

1. Electrical Circuit Design: Prior to making any purchases, it was advisable to thoroughly consider the requisite capabilities of the device, as well as any additional functionalities to be incorporated, in order to facilitate the design of the circuitry.

2. Selection of electrical and mechanical components: Following the completion of the design phase, the subsequent step involves the selection of the necessary components for construction. For instance, in order to modify the rotational speed of a motor or in our case, the amount of power delivered to the heating element, the inclusion of a transistor or Metal–oxide–semiconductor field-effect transistor (MOSFET) was essential. This component functions as a switch, regulating the power supplied to the motor and thereby facilitating changes in its speed.

3. Code writing: In the process of constructing a portable device, a critical stage involves the selection of a microcontroller and its subsequent programming to enhance the device's autonomy and user-friendliness.

4. Checking for energy consumption: It is a crucial consideration in the design of portable electric devices. Engineers must ensure that these devices operate for a sufficient time. To achieve this, engineers need to calculate the energy consumption and may need to replace certain components or increase the battery storage durability.

5. Designing the device: Once all the necessary components have been selected and assembled, the device can be rendered using a 3D modeling software.

When implementing the aforementioned procedures in our study, we engage in the selection of various mechanisms present in each heating element, such as the Negative Temperature Coefficient (NTC) and heating cartridges. Additionally, we conducted simulations of different geometries for the heating block, which consists of the heating element and the material responsible for accommodating a 0.5 mL eppendorf reaction tube. Furthermore, we devised strategies for temperature control. The simulations were made by primarily making several models with the help of Computer-aided design (CAD) software and subsequently by running heat propagation simulation with a cloud-base software. They were reported in simulations with multiple liquid volume levels. The present study also explored the components and programming utilized to ease user interaction within the LAMP portable equipment.

Additionally,the detection method employed in LAMP was also researched. From the methods available, these encompass various types of detection, such as turbidity and colorimetric assays, where we focused on the last one.

The procedure for performing LAMP assays is illustrated in Figure 1.2. Initially, a sample is collected from a specific area of interest, in this case, seawater from a public beach. The sample is then passed through two filters, namely the pre-filter and the main filter. Subsequently, the membrane filter is placed inside a test tube containing the LAMP mixture. The entire assembly is then incubated in the device at a temperature of 65°C for a duration of 30 minutes.

At the end of this incubation period, the test tube is inverted to allow the liquid to come into contact with a small paper insert located at the top of the tube. This paper insert is impregnated with Zn-MX and serves to change the color of the assay from yellow to pink if the test result is positive. Detection based on the strategy in ref [26].

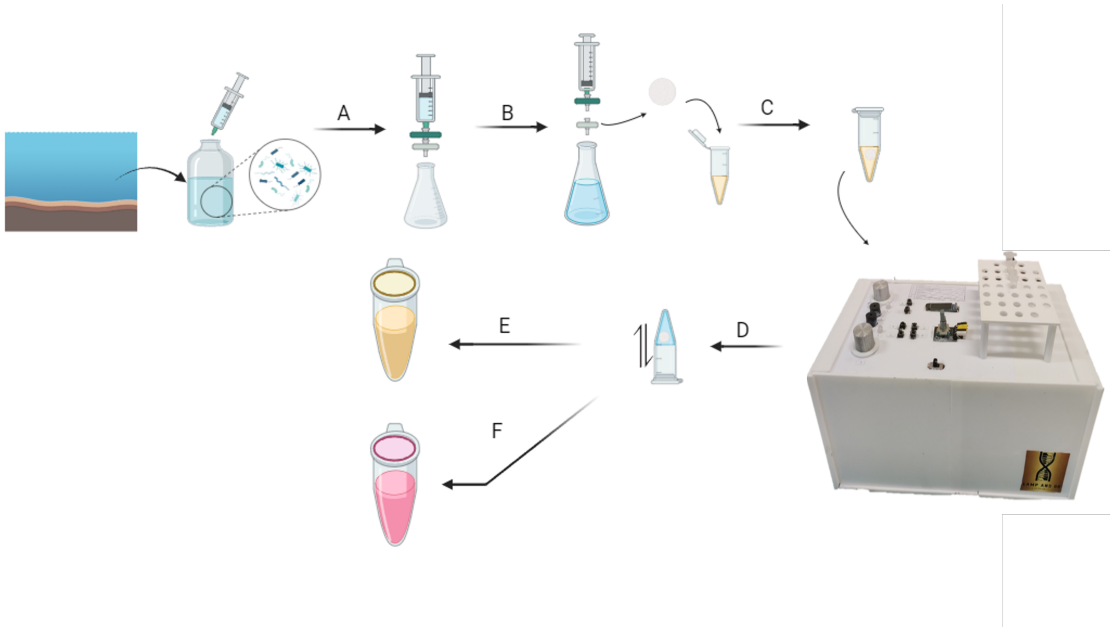

Figure 1.2: Procedure made to perform a LAMP assay, where A) the test sample is collected and passed through a pre-filter and a filter, B) the membrane filter is then removed from the structure that holds it and is placed in the test tube, C) placement of the tube inside the device built for 30 minutes at 65 °C, D) removal of the tube and its inversion, where the result could be E) yellow if negative or F) pink if positive. The present scheme was created with biorender.com

The proposed device of this thesis has the necessary equipment to conduct LAMP assays successfully, with the most efficient approaches to make it easier and less expensive to construct in short periods of time, as well as the ability for both skilled and inexperienced personnel to perform the assay. In addition, it will be constructed in a customised device box that can contain all the necessary instruments and reagents for performing the assay without the risk of contamination, as well as safely store the electronics.

2

Materials and methods

This chapter provides a comprehensive overview of the materials and methods employed in the study. It starts with a discussion of the simulation process, including an examination of the software utilized for designing and simulating heat propagation, as well as emulating certain circuitry. Subsequently, specifications regarding the heating chamber are presented. Additionally, a detailed inventory of the components employed in constructing the circuit is provided. The protocols employed for measuring power consumption and heating time will be outlined, followed by a description of the temperature sensor calibration process. Finally, the construction of the box itself, a filtration structure and the selection of components for the LAMP assay are presented.

2.1 Simulation

The entire Computer-aided design (CAD) project, including the design of the heating chambers and the device, was carried out using the software Shapr3D (Budapest,Hungary).

The study also included conducting simulations using the cloud-based analysis platform SimScale (Munich,Germany). These simulations aimed to determine the optimal heating chamber for reaction tubes, taking into account scenarios with different volumes of liquid inside the tubes.

The software possesses the capability to effectively address problems of varying degrees of complexity, exhibiting a notable degree of precision, while not requiring substantial computational resources. This was achieved through the use of Finite element analysis (FEA), which enables the resolution of intricate heat transfer issues by partitioning them into smaller components [34, 35]. Finite element analysis (FEA) is a computational method used in engineering and applied sciences to approximate and analyze the behavior of complex systems. The initial simulations were done in the absence of water and subjected to "Heat Transfer Analysis". The main purpose of this analysis was to ascertain the temperature distribution and heat flux within a solid model, without considering any heat exchange between two bodies. Following this, the simulation was carried out utilizing the "Conjugate heat transfer v2.0"feature within the SimScale software, where

heat exchange takes place at the interfaces and is transferred through conduction in solids and convection in fluids. Figure 3.1 A) illustrates a heating chamber that has been constructed by perforating a hole with dimensions of 3 cm in height and 1 cm in diameter at the centre of an aluminum rod measuring 5 cm in height and 2 cm in diameter. The lower section of the chamber has been filled with Loctite epoxy (Düsseldorf, Germany) to shape the bottom of the reaction tube structure. The fabrication method initially proposed for one of the configurations studied (Figure 3.1 B) involved the use of e epoxy to form the cylindrical structure. However, due to the inability to run the simulation with epoxy, the material was subsequently changed to aluminum.

The circuit simulation software Tinkercad (San Francisco,United States) was employed to enhance the efficiency of circuit determination, thereby minimizing the risk of component damage and expediting prototype construction [36]. The facilitation of the interaction between the microcontroller Arduino (Scarmagno, Italy) and its associated components was also enabled.

2.2 Device build

2.2.1 Circuit build

The components used to build the circuit of the device are listed in table 2.1, where some of them are visible in Figure 3.3.

The UNI-T utp3702s bench power supply (Dongguan, China), was initially used to regulate the power supplied to the heating element and assist in selecting a power bank with the appropriate capacity and voltage level.

A Hewlett Packard 34401a desktop digital multimeter (Palo Alto, United States), was used for evaluating and troubleshooting any components that required testing. Additionally, a soldering iron was utilized for soldering the wires that connected each component.

Some of the components are interchangeable, such as using an Liquid crystal display (LCD) instead of an Organic light-emitting diode (OLED) display. The Arduino Mega (Scarmagno, Italy) was programmed using an open source IDE provided by the manufacturer.

2.2.2 Sensor calibration

As the sensor was not positioned inside the reaction tube, it required calibration. This calibration process involved recording NTC 100k thermistor sensor measurements at 10-second intervals. These measurements were taken in a 2.5 cm deep hole that had been drilled into the bottom aluminum chamber. The calibration procedure was conducted by comparing the thermistor sensor readings with those obtained from a thermometer sensor placed inside the reaction tube, as illustrated in Figure 2.1 B). The depth of this hole was selected to ensure that the sensor was situated as close as possible to the location of the liquid inside the reaction tube.

Table 2.1: Circuit materials

Component	Quantity
Relay	1
Switch	1
12 V 5 A power supply	1
20000 mAh Power Bank	1
100 Ω resistor	2
240 Ω resistor	4
680 Ω resistor	2
1 KΩ resistor	11
2.2 KΩ resistor	2
10 KΩ resistor	1
100 KΩ resistor	2
IRF 520 MOSFET module	2
24 V 50 W cartridge heater	2
Arduino Mega	1
Button	6
Rotatary encoder	1
LED	6
Buzzer	2
NTC 100K thermistor	2
OLED display	1
Breadboard	1
Bench power supply	1
Desktop multimeter	1
Soldering iron	1

Afterwards, a calibration curve was constructed to determine the corresponding relation. All readings were taken from room temperature to working temperature (65 °C). The experiment was conducted under two conditions. The first condition involved testing before the components were placed inside the box, using liquid volumes of 0.2 mL, 0.1 mL, and 0.0 mL. During this phase, the heating chamber (aluminum cylinder) was suspended in the air using a claw. The second condition took place after the components had been situated within the box, with a liquid volume of 40 μL. This volume is the same as a normal LAMP assay. In the last case, the thermometer sensor utilized within the reaction tube was substituted with an Negative Temperature Coefficient (NTC) 100K thermistor that was embedded with epoxy for enabling its operation in an aquatic environment (Figure 2.1 A). Additionally, an extra layer of polyethylene material was incorporated around the aluminum cylinder to enhance the isolation of the heating chamber.

2.2.2.1 Heating time

The time required for each heating chamber to reach the desired temperature is a criterion to consider, as the device must be rapidly prepared for assays. To measure it, a chronometer to mark the measurements in the sensor calibration assay is used to count the time to

rise from ambient temperature (22 °C) to the goal temperature (65 °C). This assay was conducted both before and after the components were placed inside the box.

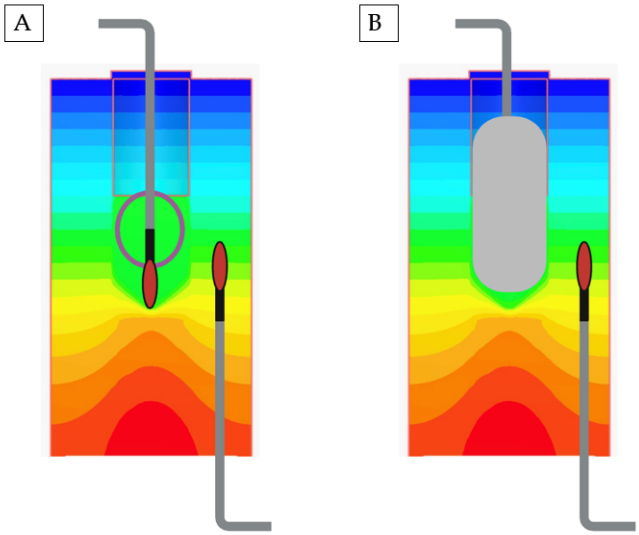

Figure 2.1: Sensor positioning, A) when the device was fully assembled, and the calibration was performed using the NTC 100k thermistor and B) when the aluminum cylinder was suspended in the air using a claw, and a thermometer sensor was employed

2.2.3 Power consumption

The power consumption of the device under various conditions, including idle mode and when using one or both chambers, was evaluated by establishing a connection between the desktop multimeter and the power bank's output in a series configuration. Subsequently, the multimeter was set to measure the current. All measurements were conducted using a voltage of 12 V. Subsequently, to validate the theoretical findings, a series of consecutive 30-minute assays were performed, with a 10-minute interval between each assay, continuing until the power bank was entirely depleted of power.

2.3 Box construction

The design of the box was created taking advantage of the software application Shapr3D (Budapest,Hungary). Subsequently, the object was divided into multiple components to accommodate the spatial constraints of the construction area of a 3D printer, as per the specifications provided by the company Varishapes (Viana do Castelo, Portugal). All components, with the exception of the support chambers and adjacent pieces (specifically, parts_resized_3_support chamber n1, parts_resized_3_support chamber n2, parts_resized_3_floor 2 n1, and parts_resized_3_floor 1 n1, available in the link "Box 3D models"in appendix A), were manufactured using Polylactic acid (PLA) as the primary material. The support chambers were constructed from Acrylonitrile Styrene Acrylate (ASA), while the adjacent pieces were made from Polyethylene terephthalate glycol (PETG). This

selection was based on the glass transition temperature coefficient. ASA was chosen as a material to accommodate the heating chamber, since it has a glass transition temperature coefficient of 112 °C. Components that are attached to the ASA materials, do not need to have such high glass transition temperature, since some temperature is dissipated before reaching it. Although it can't be PLA since its coefficient is of 60 °C, which means this material cannot be positioned near the heating system. Therefore PETG was selected for having a value of 85 °C.

2.4 Filtration

The software Shapr3D was employed to design a supporting structure for accommodating a 6 mm diameter filter membrane (Durapore®) with a pore size of 0.45 μm to make it compatible with a syringe system for sample filtration, as illustrated in block B of Figure 2.2. Subsequently, these supporting structures were 3D printed by the company Igus (Cologne, Germany), using iglidur® i8-ESD material.

Figure 2.2: Filtration system composed by A) an pre-filter and B) a filter

In order to assess the stability and integrity of the filter, a series of experiments were conducted involving the passage of water using a syringe. A pre-filter CHROMAFIL® Xtra PET, 25 mm, 1 μm (Nordrhein-Westfalen, Germany) was employed for the purpose of separating larger constituents present in seawater. To assess the endurance of the described pre-filter, a series of ten consecutive 25 milliliter syringes containing seawater were utilized, with intervals of 2 minutes between each syringe. Following this sequence, a 20 minute break was made. This sequence was made until the time of the assay was considered to be above optimal (*e.g.* 15 seconds).

2.5 LAMP assays

The $ZnCl_2$-Murexide (Zn-MX) detection ensemble was prepared by mixing equal volumes of 10 mM $ZnCl_2$ (Sigma-Aldrich) to 5mM Murexide (Sigma-Aldrich). Grade 4 Paper Whatman® (Sigma-Aldrich) was cut to 8 mm and 4 μL of Zn-MX was placed on its surface and left to dry for at least 5 min (until the color changed from orange to yellow). The papers with Zn-MX were placed inside the lid of 0.5 mL PCR tubes (Axygen) to which the LAMP reaction mixture was added.

The LAMP reaction mix was prepared in a total volume of 40 μL containing the following components: 16 U *Bst* (enzyme units *Bacillus stearothermophilus*) 2.0 (NEB), 1x

Isothermal Amplification Buffer (NEB) plus 4 mM $MgSO_4$ (NEB); 1.4 mM each dNTP (NZYTech) and 1× primer mix (1.6 μM FIP/BIP primers; 0.4 μM LF/LB primers; 0.2 μM F3/B3 primers (STABVida) ENT [37]).

Enterococcus faecalis cells were resuspended in water and quantified with a spectrophotometer. The solution was diluted following the pre-determined conversion factor that 1 $O.D._{\cdot 630nm}$ corresponds to $5.8x10^2$ colony forming units (cfu)/ μL in order to obtain a final concentration of 50 cfu/μL to spike the filter membrane. 2 μL of this cell suspension was placed in a 0,45 μm PVDF filter membrane (Durapore®), cut to 6 mm diameter. The filter with bacteria was added to the rection mixture and incubated at 65°C for 30 minutes in a thermocycler with heated lid at 65°C or in the portable device with the same conditions. The previous approach was also tested to *Escherichia coli*, with a final concentration of $50x10^2$ cfu/μL.

The tubes were removed from the incubators, inverted and pictures were taken in a scanner at the indicated time points after inversion.

3

Results

This chapter presents a comprehensive overview of the findings related to the assays discussed in chapter 2. The CAD models are provided along with their corresponding dimensions. Subsequently, simulations are conducted to analyze the heat propagation in the presence and absence of fluids. The fundamental electronics were then modeled using an online software. A circuit diagram depicting the final assembly is featured. Additionally, the calibration of the temperature sensor and the recorded time taken for heating from room temperature to the desired operating temperature are described. The anticipated and observed power consumption values are reported. Detailed information regarding the construction of the case is provided. The protocol for filtering seawater is outlined. Finally, the outcomes of laboratory LAMP assays are presented.

3.1 Simulation

3.1.1 CAD models

To accurately replicate the heating capabilities of the elements, models of both the elements themselves and the heating chambers were constructed. The CAD models are of two types of heating elements, namely a 3D printer cartridge heater and a nichrome wire.

Figure 3.1 illustrates the three configuration models that were examined. In Figure 3.1A, a cartridge heater is positioned underneath the location where the reaction tube is situated. This heater is enclosed by an aluminum cylinder measuring 20 mm in diameter and 50 mm in height. Figure 3.1B depicts the utilization of epoxy as the material for constructing the cylinder, and a nichrome wire is positioned around the reaction tube. The diameter measures 20 mm, while the height is recorded as 31 mm. In Figure 3.1C, a comparable methodology to that of Figure 3.1A is employed, albeit with a modification in the placement of the heating element. Specifically, the heating element is positioned adjacent to the reaction tube, resulting in a geometry characterized by a diameter of 33 mm and a height of 31 mm. From now on this models will be reference as model A,B and C respectively.

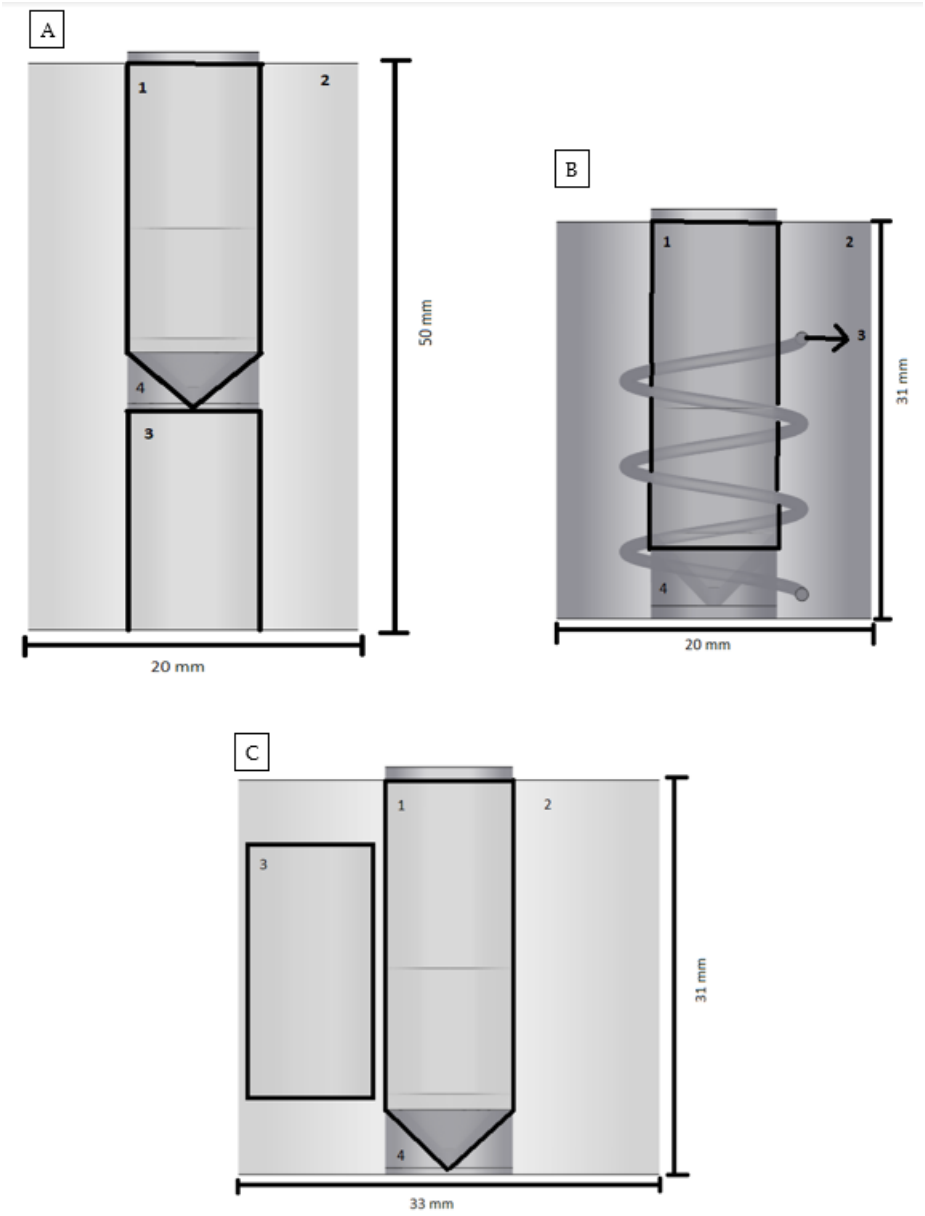

Figure 3.1: A) Cartridge heating where 1 is the Eppendorf reaction tube, 2 the aluminum block, 3 the heating element (Cartridge) and 4 is epoxy, B) Nichrome wire heating, where 1 is the reaction tube, 2 the epoxy mold, 3 the heating element (Nichrome wire) and 4 is epoxy, C) Side cartridge heating where 1 is the reaction tube, 2 the aluminum block, 3 the heating element (Cartridge) and 4 is epoxy

3.1.2 Simulation of heat propagation

After constructing the model, it was crucial to ensure that the temperature within the heating chamber, particularly on its inner walls, is uniform to facilitate the successful execution of the LAMP assay. It was fundamental to ensure that the temperature does not surpass the recommended thresholds for each material, as this could result in the loss of their inherent properties. Figure A.2 illustrate the results of simulations performed using SimScale. The simulations involved applying insulation throughout the chamber,

preventing heat loses, except for the top region where a room temperature of 20 °C was assumed. The objective was to ascertain the temperature of the chamber walls in the absence of an insulation cap. It was projected that each heating element would present a surface temperature of 80 °C. The model that had a higher temperature employed a coil heater. Neither of them surpassed the fusion temperature of aluminum, which is 660 °C. In order to achieve a working temperature of 65 °C within the reaction tubes, an additional simulation was conducted (Figure 3.2). This simulation involved the use of a partially insulated cap, which was enhanced with an additional layer of aluminum. As a result, the average temperature imposed on the top surface of the cap was approximately 40°C. Furthermore, the realism of the simulation is enhanced through the incorporation of the reaction tube and the application of an epoxy filling at the base of the cavity to shape the bottom of the tube. Water was employed as a substitute for the LAMP mixture. Figure 3.2 illustrate the equilibrium temperatures achieved during the LAMP test when each element generates an equal amount of power. The findings suggest that employing a cartridge heater positioned at the base of the reaction tube leads to an augmentation in the mean temperature readings within the enclosure. All the CAD designs can be consulted in appendix A, "3D Heat Models".

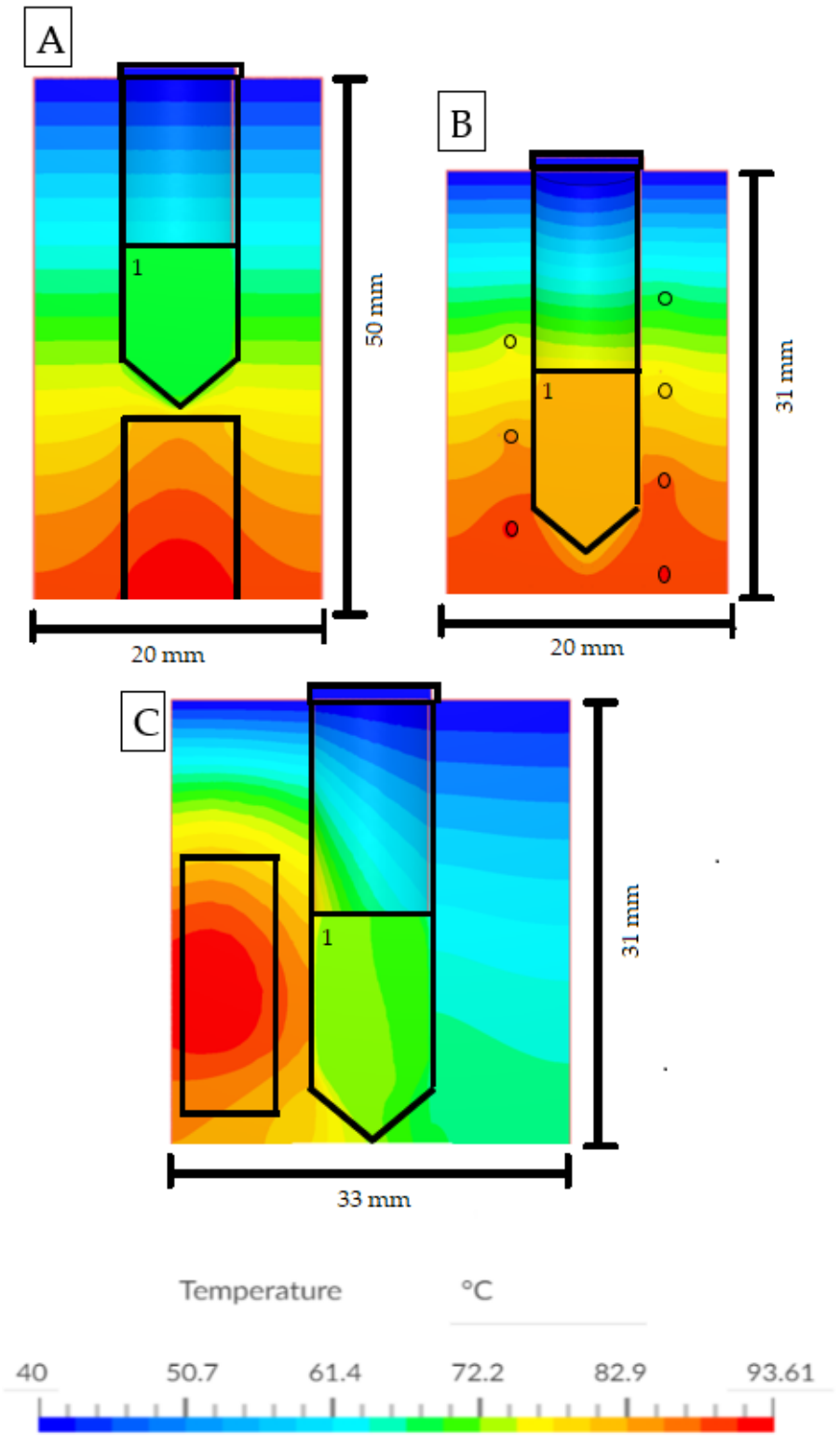

Figure 3.2: Simulation of the reaction mixture temperature A) with Cartridge heating configuration, B) With a nichrome wire heating configuration and C) with a cartridge heating from the side configuration. "1"represents the water inside the tube

3.1.3 Electronics modeling

Simulating circuitry is a recommended step to do, since it can prevent components to be damaged during the test phase, accelerate the initial steps of the build, help predict some upcoming problems, and prove the base concepts of the device.

Figure 3.3 illustrates the construction implemented on Tinkercad, represented in a diagram format. The schematic simulates the connections established from the temperature sensor to the Arduino, with the inclusion of an operational amplifier. Additionally, a TIP 120 transistor was incorporated to effectively regulate the power supply from the battery to the heating element, ensuring the Arduino remains unharmed. Moreover, the diagram features two LEDs, namely a red LED and a green LED, which illuminate when the temperature falls below or exceeds 65 °C, respectively. Additionally, the diagram depicts the interconnections with an LCD display, which serves to visually represent the present temperature in the simulation.

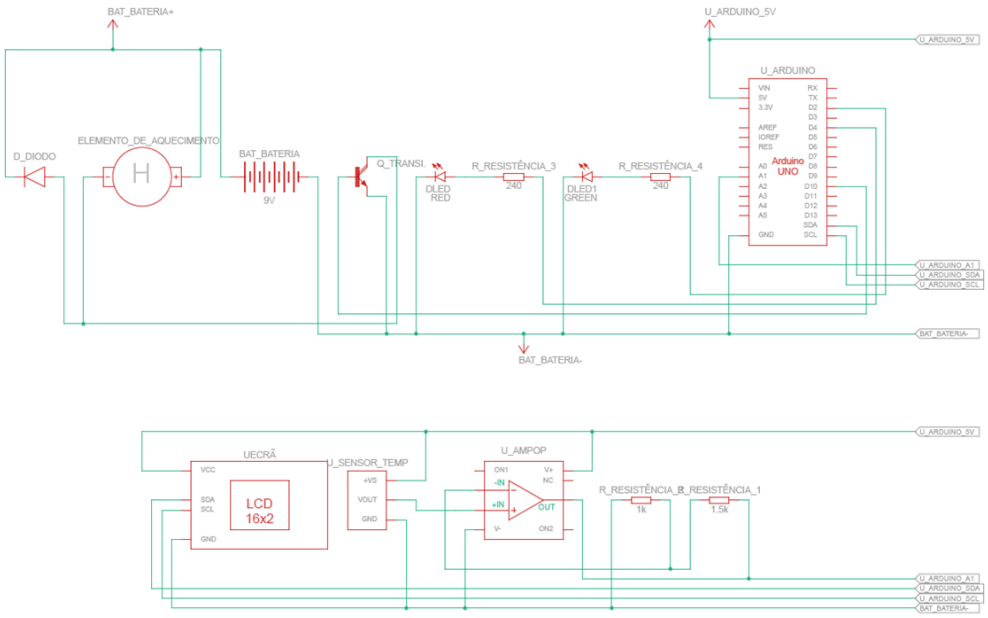

Figure 3.3: Circuit simulated in Tinkercad software

The code for this simulation was initially developed to control the aforementioned components. Subsequently, the final code was constructed, taking into account the insights gained from this initial code, along with some optimizations. The Tinkercad code can be found in a GitHub page (url located in appendix A). Furthermore, an additional visually descriptive representation of the circuit can be observed in Figure A.1.

3.2 Device build

3.2.1 Circuit Build

After testing each component, the final circuit was constructed, and it is depicted in Figure 3.4. Block A represents the power delivery system, B the heating elements and the IRF520 module, C all the Light emitting diode (LED), buzzers and the rotary encoder, D all the navigation buttons, E the temperature sensors, and F the OLED screen.

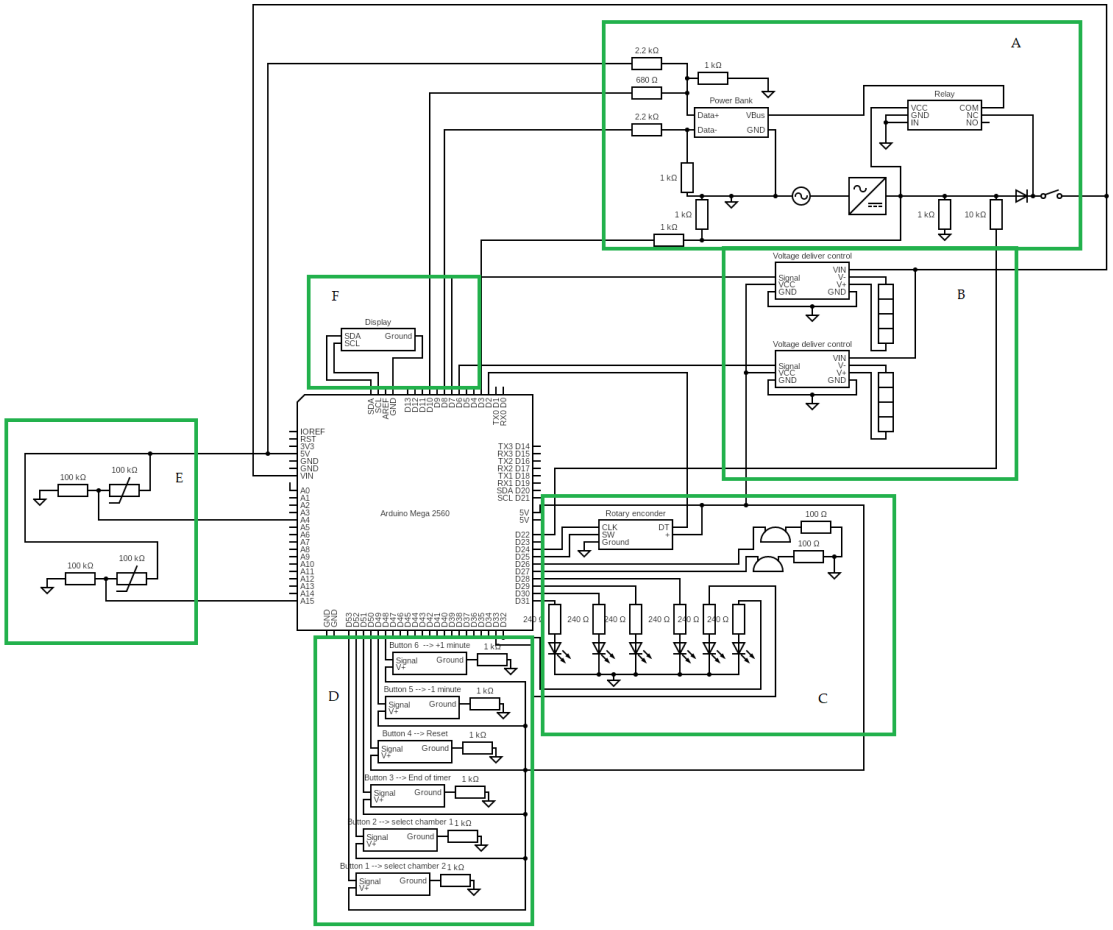

Figure 3.4: Final circuit build presented in block where, A) presents the power delivery system, B) heating elements and the IRF520 module, C) Light emitting diode (LED), buzzers and the rotary encoder, D) navigation buttons, E) temperature sensors, and F) the OLED screen.

3.2.2 Sensor calibration

The graphs from Figures 3.5 to 3.9 represent the temperatures recorded in the sensor located in the 2.5 cm deep hole drilled in the bottom of the aluminum chamber and the thermometer placed inside the reaction tube, as well as their relation with different volumes of water (0.2 mL, 0.1 mL and 0.0 mL) inside it. The measurements has been performed in the experimental setup mentioned in chapter 2, subsection 2.2.2, **with all the components (*e.g.* aluminum cylinder, sensors, Arduino) outside the box**.

The graphs from Figures 3.10 and 3.11 represent the temperatures recorded in the sensor located in the 2.5 cm deep hole drilled in the bottom of the aluminum chamber and the thermistor placed inside the reaction tube, with a liquid volume of 40 μL, the same amount the LAMP assay has, as well as their relations with inside it, **with all the components already inside the box**.

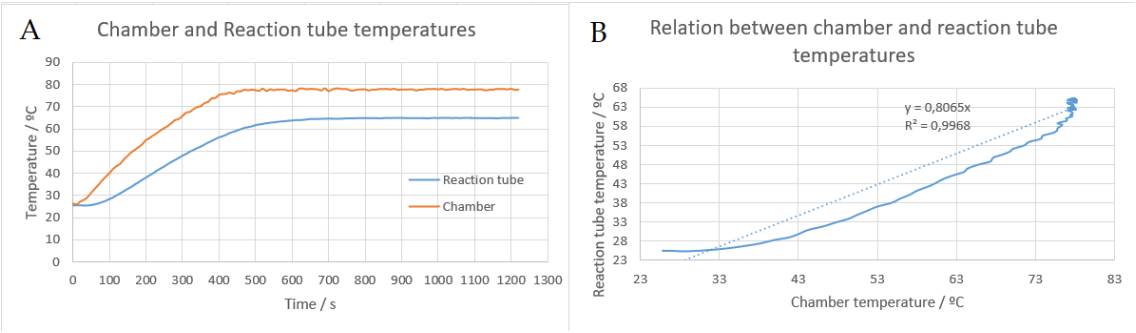

Figure 3.5: A) Chamber and reaction tube temperatures along time in chamber 2 with 0.2 mL of liquid and B) their respective relation

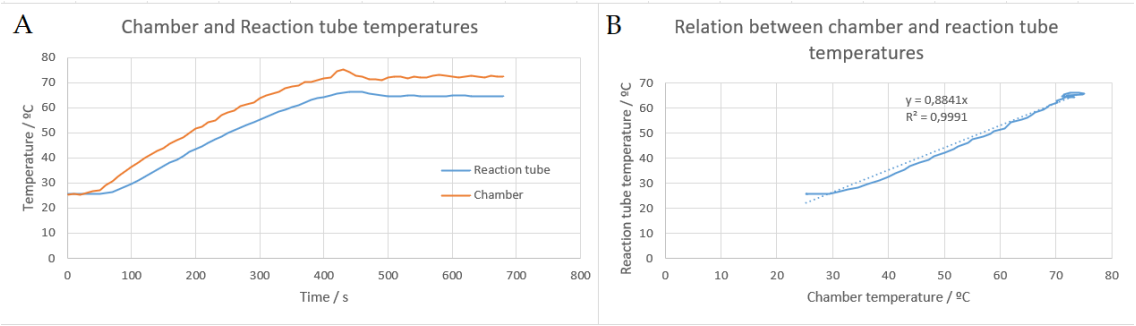

Figure 3.6: A) Chamber and reaction tube temperatures along time in chamber 1 with 0.1 mL of liquid and B) their respective relation

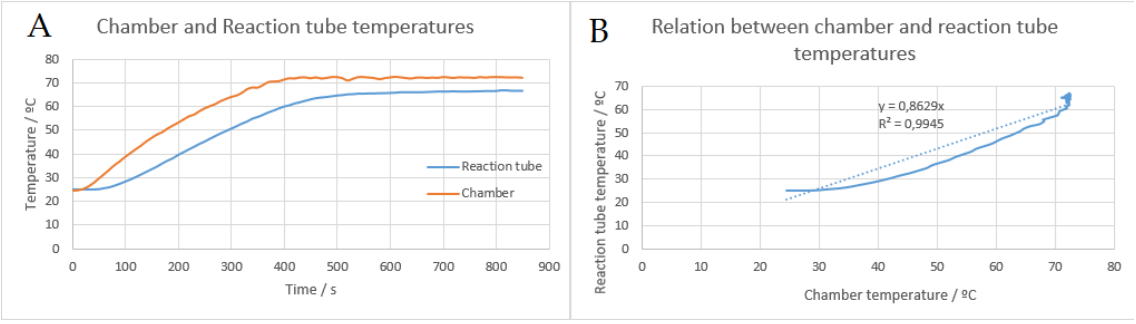

Figure 3.7: A) Chamber and reaction tube temperatures along time in chamber 2 with 0.1 mL of liquid and B) their respective relation

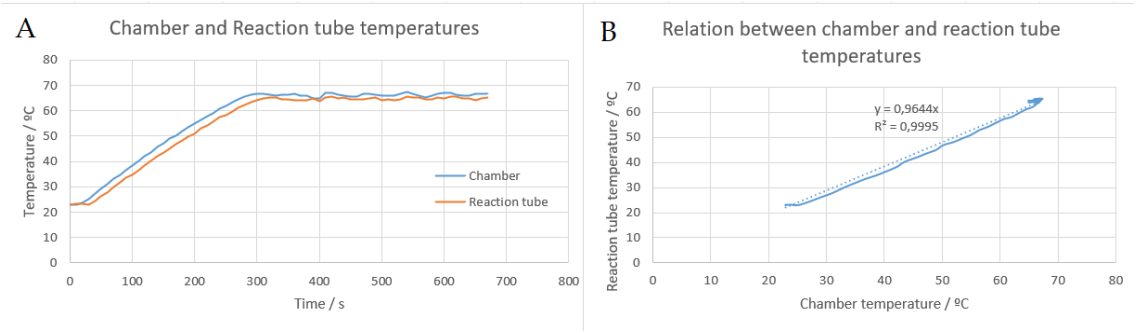

Figure 3.8: A) Chamber and reaction tube temperatures along time in chamber 1 with no liquid volume in the reaction tube and B) their respective relation

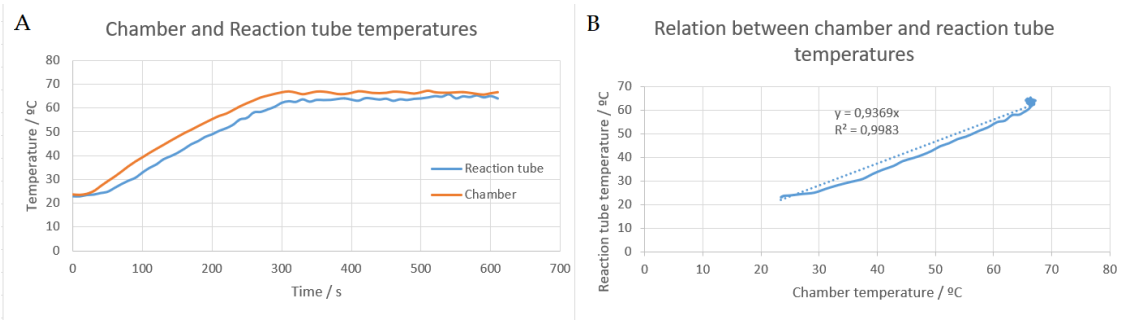

Figure 3.9: A) Chamber and reaction tube temperatures along time in chamber 2 with no liquid volume in the reaction tube and B) their respective relation

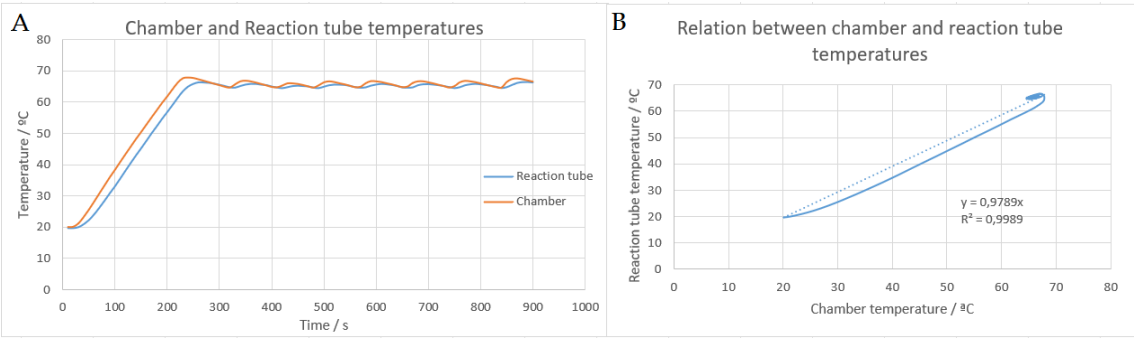

Figure 3.10: A) Chamber and reaction tube temperatures along time in chamber 1 with 40 μL liquid volume in the reaction tube and B) their respective relation

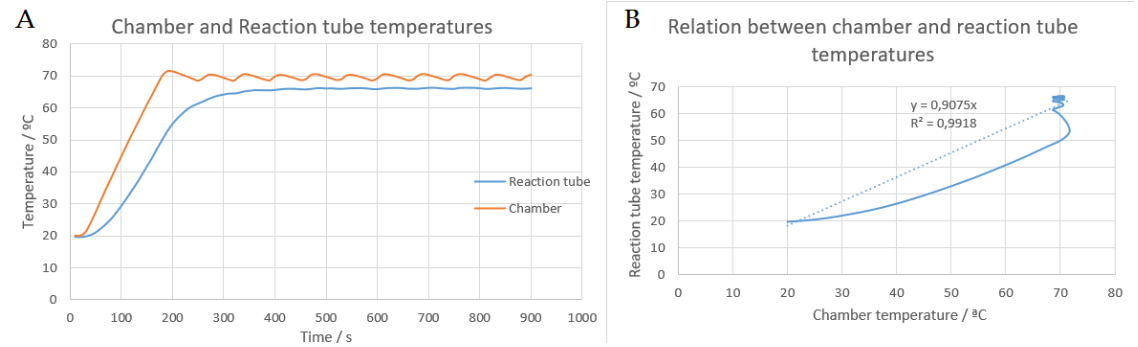

Figure 3.11: A) Chamber and reaction tube temperatures along time in chamber 2 with 40 μL liquid volume in the reaction tube and B) their respective relation

3.2.2.1 Heating time

The time taken for each heating chamber, suspended in the air by a claw outside the box, to reach the target temperature of 65°C from room temperature was approximately 8.5 minutes when the reaction tube was filled with a liquid volume of 0.2 mL, 7.5 minutes with 0.1 mL, and 5 minutes when no liquid was used. These times remained consistent when utilizing one or both chambers simultaneously.

Once all the components were positioned inside the box, the time required for 40 µL to reach the desired temperature was approximately 3.5 to 4 minutes.

3.2.3 Power consumption

When operating at a voltage of 12 V, the device drew 81 mA from the power source in standby mode. When one chamber was active, it drew a current of 800 mA, and when both chambers were active simultaneously, the current drawn was 1420 mA.

During the utilization of both chambers and conducting consecutive assays with a 10-minute break between each, the 20000 mAh power bank was exhausted after completing 10 LAMP tests.

3.3 Box construction

To accommodate all the necessary components to perform a portable LAMP assay, the box was designed with dimensions of 15 cm by 26.4 cm by 15.77 cm. It featured three levels: the first level had a height of 4.5 cm, creating a space for the power bank and the power supply. The middle level, with a height of 5.9 cm, was allocated for the circuitry, including the Arduino and all associated cables, as well as the heating chambers, which were housed in cylindrical structures with corresponding fittings. These structures are visible on the left side of this level, as depicted in appendix A Figure A.5. The upper level included openings to accommodate user-accessible components, caps for the heating chambers, and a support for holding reaction tubes.

Each floor and the back wall had a thickness of 0.4 cm, while the lateral walls were constructed with a thickness of 0.6 cm to ensure adequate weight-bearing capacity. Additionally, the box was equipped with a cover, although it is not visible in Figure A.6 of appendix A. This figure presents the final build of the device, offering a top view showcasing all user-accessible components and a side view where the logo "LAMP and Go; a quick and portable solution", is clearly visible. Detailed 3D models of all the parts of the box can be accessed through the link provided in the "Box 3D models"section of the appendix.

3.4 Filtration

A structure for holding the filter membrane was designed using CAD software, as depicted in Figure 3.12. Detailed models of this structure can be found in the "3D Filter model"section of Appendix A. The structure, with a extend diameter of 9.6 mm, had an inner ring of 4 mm radius to accommodate the filter membrane (Durapore®), which had a diameter of 6 mm. At the bottom part, there are a total of fourteen apertures measuring 0.6 millimeters in diameter, which allow the passage of the liquid. In order to seize it, the aforementioned structure was equipped with a cover, which is visually depicted on the right side of Figure 3.12. This geometry and dimensions of the structure were used to adapt them to a filter holder, that was originally made to fit 10 mm membrane filters (Figure A.4 depicts the original filter). The structural design effectively demonstrated its ability to securely contain the filter, preventing any displacement or damage during operation.

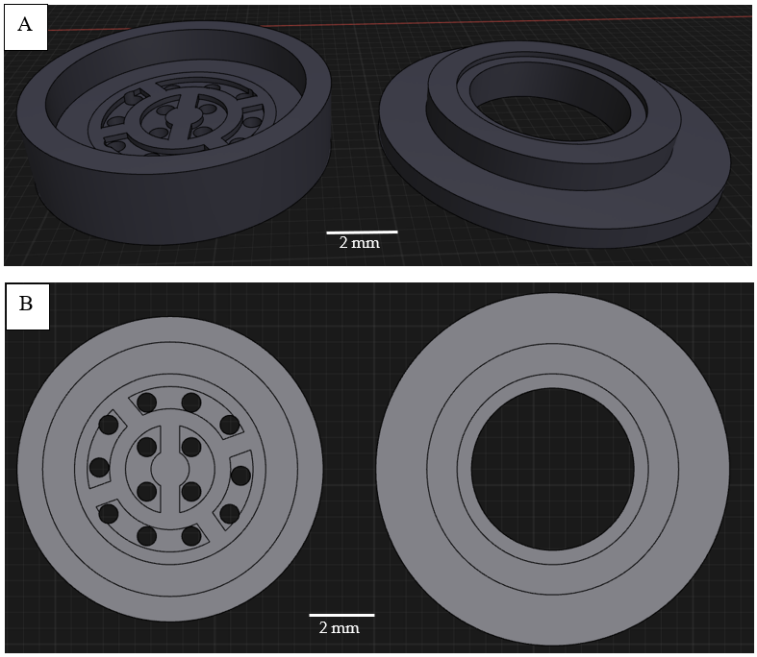

Figure 3.12: Structure where the membrane filter will be placed in order to be able to be used with the syringe system, in A) a view from a side is displayed while in B) is a view from the top

Figure 3.13 illustrates the steps that the user should follow to utilize the filtration system. The initial step involves inserting the membrane filter into the designated structure and securely positioning it within the filter holder. Following this, it is attached to the pre-filter, and the testing process can commence. Regarding the pre-filter durability, Table 3.1 provides the duration in seconds required for each filtration of 25 mL of seawater collected from Carcavelos Beach at 10:00 am on the same day as the assay. The water did not appear to contain algae or be significantly dirty.

Figure 3.14 illustrates the pre-filter both before its initial use and after each 20-minute break during the testing process.

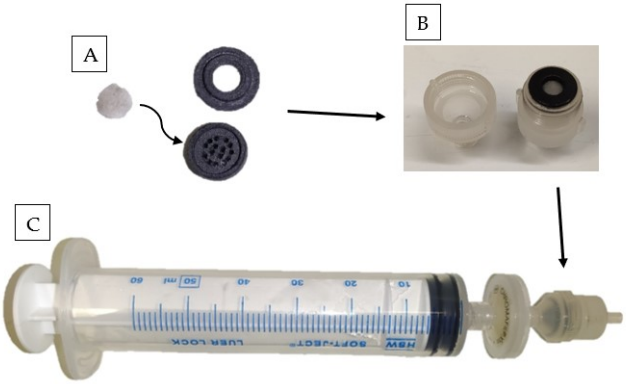

Figure 3.13: Guide of how to mount the filter in the syringe, by A) insert the membrane filter in the structure built in the 3D printer, B) placing it in the filter holder and C) screwing in the end part of the pre-filter, which is attached to the syringe

Table 3.1: Pre-filter filtration time of 25 mL of sea water of Carcavelos beach in consecutive tests within 2 minute intervals. After 10 tests a break of 20 minutes was made

Test	Time /s	Test	Time /s	Test	Time /s
1	5	11	7	21	7.5
2	5	12	6.5	22	6.5
3	6	13	7.5	23	7
4	6	14	6	24	7
5	5.5	15	6.5	25	7.5
6	5.5	16	7	26	7.5
7	6	17	7	27	8.5
8	6	18	7.5	28	7
9	5.5	19	6.5	29	8
10	6	20	6.5	30	8.5

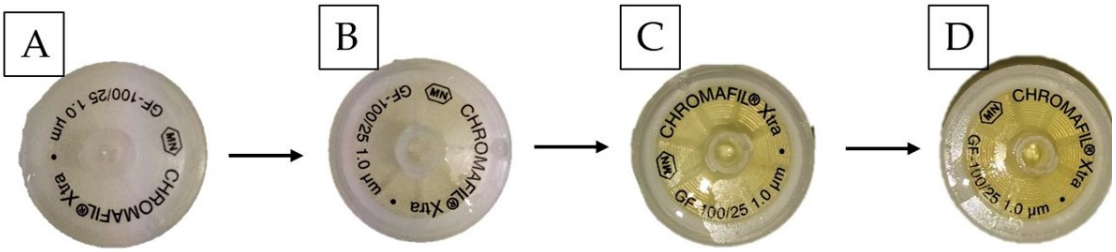

Figure 3.14: Pre-filter evolution with the number of tests, A) before any test, B) after 10, C) 20 and D) 30 tests

3.5 LAMP assays

In order to test if the device heated at the right temperature, two LAMP assay were made in parallel, one using the prototype and other the thermocycler. All the other conditions, from the LAMP reaction mixture to the spike of the filters were done as said in section 2.5 of chapter chapter 2. After the tubes were inverted, Figures 3.15, A.7 and 3.16 an assay

made with *Enterococcus faecalis* and two with *Escherichia coli* respectively. In order to proof the versatility of the LAMP device, an assay with *Candida albicans* was made (depicted in Figure A.9).

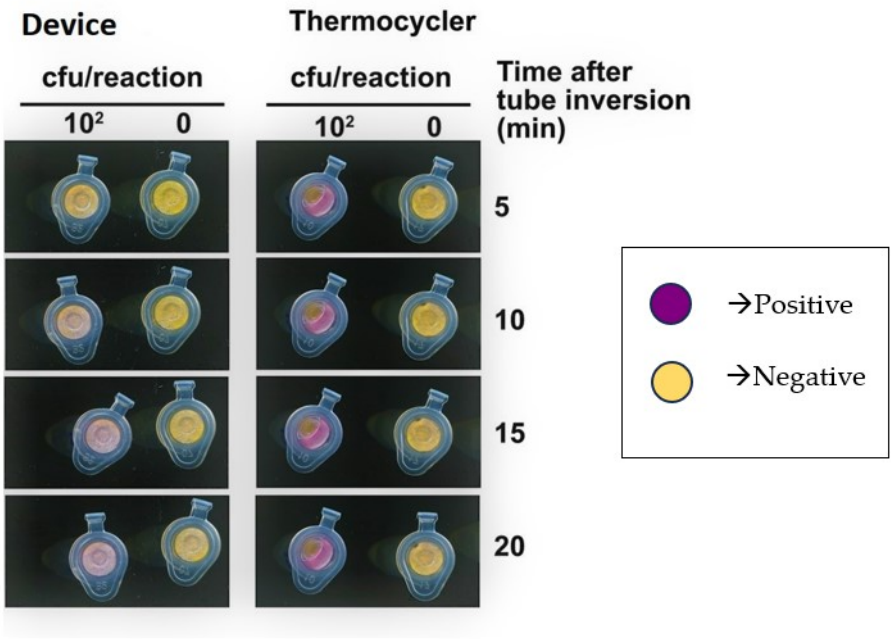

Figure 3.15: LAMP assay of *Enterococcus faecalis* in the portable device and the thermocycler

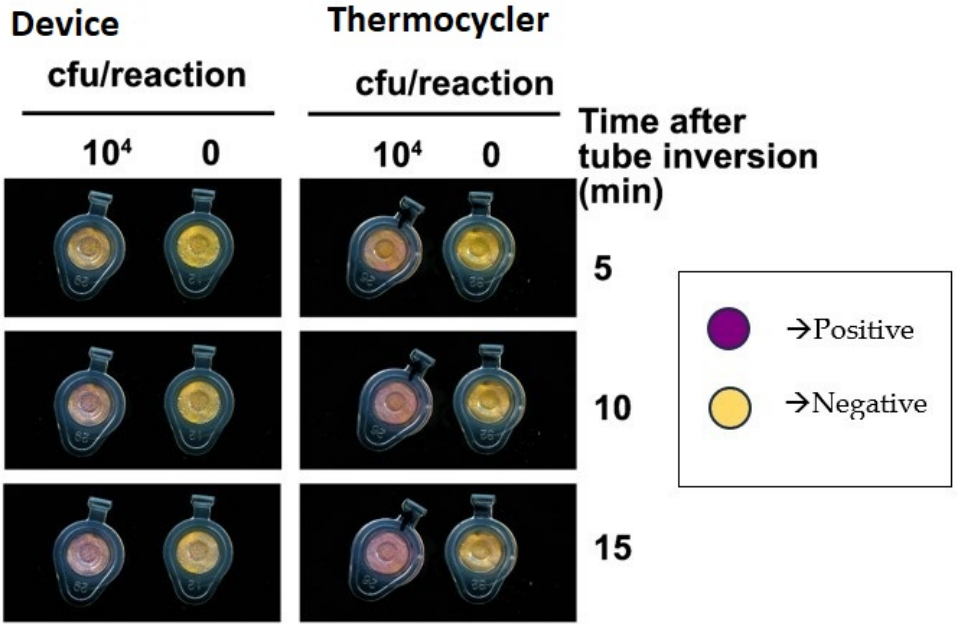

Figure 3.16: LAMP assay of *Escherichia coli* in the portable device and the thermocycler

4

Discussion

This chapter presents the discussion regarding the results presented in chapter 3. The initial focus of the discussion pertains to the outcomes derived from the simulation, encompassing aspects such as the employed geometries and the propagation of heat. Subsequently, attention is directed towards the circuit, including the construction of the code, control of power delivery, utilization of temperature sensors, their calibration, and the assessment of power consumption. The discussion also includes the filtration system, providing rationale for the selection of filters and the underlying reasons for this decision. The interpretation of the results obtained from the LAMP assay is finally conducted.

4.1 Simulation

Simulations were conducted using SimScale, a cloud-based computing service, to ascertain the most suitable placement of the heating element within the chamber.

There were studied 3 possible geometries of the incubator chambers, distinguished by models A,B and C (visible in Figure 3.1).

In reference to the outcomes obtained in the absence of water, as illustrated in Figure A.2, it can be observed that model B effectively maintained the interior wall temperature at a consistent level with that of the heating element. Following this, model A also exhibited a good temperature distribution, with colder areas unable to affect the assay due to the low volume of liquid inside the reaction tube, which would consequently be situated in the hotter regions. Model C performed the worst, as the temperature gradient in the walls in contact with the reaction tube was the coldest when compared to the previous models. As indicated in Chapter 3.1.2, the epoxy mold was replaced with aluminum in the simulations due to the fact that the epoxy values presented in the software were tailored for conventional uses of the material as electrical and thermal insulation, rendering it unsuitable for the simulation [38].

Aluminum was chosen as a suitable material for heating purposes in DNA amplification methods, such as PCR, due to its well-established effectiveness. This decision was influenced by the material's remarkable properties, which include high specific heat

capacity, latent heat of fusion, and thermal conductivity, as well as its ease of machining and cost-effectiveness [39, 40].

In conducting an enhanced simulation (Figure 3.2), the primary objective was to verify if water temperature was uniformly distributed. The most suitable model utilized in this study was model A. This particular model exhibited good results since there was no temperature variation in the liquid inside the reaction tube. On the other hand, Model C showed some variation, rendering it unsuitable. This variation was likely attributed to the closer proximity of the heating element to the less isolated area. Additionally, model A offers the benefit of allowing for the replacement of the heating element without the necessity of removing the chamber, as it is not fused to it, unlike model B. Furthermore, the manufacturing process can be automated.

The initial selection of the necessary electrical components for constructing the prototype was determined through simulations using Tinkercad software.

The Tinkercad simulation allowed for the verification of specific principles related to the device. This included precise temperature measurement using a sensor provided by the software, as well as the modulation of power supplied to the heating element through the utilization of a transistor controlled by Pulse width modulation (pwm) in the Arduino socket. It's important to note that the higher the pwm value, the more power is delivered to the heating element.

4.2 Device build

To create a functional device, several steps were undertaken. These steps included building the circuit responsible for collecting data from each temperature sensor and supplying energy to one or both heating elements based on their respective values. Additionally, interactive components were incorporated to allow the user to control aspects of the assay, such as runtime, and to provide the necessary information for verifying the correct parameters, using a display and LED indicators.

4.2.1 Circuit Build

In the process of constructing the circuit, thorough research was necessary to select specific components that align with the intended purpose. This purpose includes choosing the appropriate temperature sensor for accurate temperature measurement, deciding between the Metal–oxide–semiconductor field-effect transistor (MOSFET) or Bipolar junction transistor (BJT) to provide energy to the heating element, and selecting a display that allows the user to view information under various environmental conditions. All chosen components must be compatible with the Arduino platform.

4.2.1.1 Arduino code

The microcontroller is the component with which all the components mentioned in the previous paragraphs and depicted in Figure 3.4 interact. To achieve this, a more comprehensive code was developed in the IDE environment, as described in Appendix A, under the link entitled "Final code". The Arduino code is responsible for displaying different menus on a display for each of the heating chambers. In Figure A.10, only chamber 1 menus are depicted. It also ensures the correct amount of power is delivered to each heating element in order to maintain the working temperature of 65 degrees Celsius, using readings from the temperature sensors.

To facilitate navigation through the menus, a set of six buttons is employed. These buttons serve the purpose of adjusting the timer by either increasing or decreasing its value, selecting between chamber 1 or 2, resetting the timer, or indicating the completion of an assay.

A rotary encoder was used to initiate and pause the timers, as well as to adjust the duration of the assay. This adjustment can be made before the assay starts or when it is paused. There are also buttons designed for executing this final function, which are deemed redundant since their primary purpose was to customize the interface to match the user's preferences.

Upon completion of the assay, the Arduino will activate a blue LED and emit an auditory signal. To indicate the readiness of each chamber for an assay, an additional pair of LEDs was employed. The LEDS were programmed to emit a red color when the chamber is not ready for an assay and a green color when it is ready.

The voltage values obtained from the temperature sensor can be read through the utilization of the analogue pins. Subsequently, these values can be converted into temperature measurements, allowing for the adjustment of the power supplied to the heating elements.

4.2.1.2 Power delivery control

The selection of the power source has been conducted taking in account the risk of damage to the components ensuring sufficient energy supply to the heating elements. In order to provide power to both the Arduino and the heating elements, it was necessary to establish separate connections directly to the heating elements. This is because the maximum output current of an Arduino is insufficient to adequately give power to the heating elements.

Block A depicted in Figure 3.4, assumes the responsibility of supplying power to the entirety of the device. There are two primary methods for accomplishing this task: by establishing a connection to an external power socket or by utilizing a pre-connected power bank. In order to mitigate potential harm to the power bank, a relay was employed to disrupt its electrical circuit upon the activation of a power outlet. Given that this particular device requires the activation of two heating elements, it becomes essential

to carefully select a power bank that possesses the capability to supply an adequate amount of power, thereby facilitating the attainment of the desired temperatures within an efficient timeframe. In order to accomplish this, a power bank equipped with a Qualcomm chipset was selected due to its incorporation of quick charge 2.0 technology. This particular protocol enables the charging of various devices, such as mobile phones, through the utilization of a USB A connection, accommodating different voltage levels. To establish communication with the chipset, the Arduino library QC2Control was utilized. The library's documentation provides instructions on how to establish the necessary connections between the Arduino and the chipset, specifically for the wires data +, data -, Vbus, and ground. A voltage of 12 Volts was selected in order to reduce the heating time.

The current capacity of Arduino is limited, thereby confining its application to the control of small-scale devices such as individual LEDs, OLEDs, and LCD displays. The microcontroller has the ability to transmit low-current signals to a driver board that possesses the capability to operate the heating elements. This driver employed in various applications have achieved their functionality through the utilization of devices such as Bipolar junction transistor (BJT)s or Metal–oxide–semiconductor field-effect transistor (MOSFET)s. The aforementioned electronic components are considered to be fundamental since they can controll with precision the power delivered to the heaters by just receiving diferent values of the Pulse width modulation (pwm) arduino output.

In this study, the choice between two options (BJTs and MOSFETs),the selection of a MOSFET module was made to regulate the power output to each heating element. The decision was based on the module's integrated components, which enable it to function as a switch and facilitate its installation and replacement in the event of malfunction. Additionally, the module offers advantages such as higher voltage power handling and improved input impedance.

4.2.1.3 Temperature sensor

To allow for precise measurement of temperature data, either a thermistor or a thermoresistance could be selected. However, thermistors can be significantly more sensitive [41].

They use semiconductors, materials where the resistance decreases with temperature (Negative Temperature Coefficient (NTC)) and cannot be represented by a linear equation. Equation 4.1 represents this sensor behavior,

$$R = \mathrm{R}_0 e^{\beta[\frac{1}{T}-\frac{1}{\mathrm{T}_0}]} \tag{4.1}$$

where β is a constant determined by the materials that make up the thermistor.

The semiconductors that can be used to create these sensors range from elements like silicon and germanium to composites of semiconducting metallic oxides. Not only are these materials chosen for their high sensitivity, but also for their stability.

Several studies have demonstrated that other thermistor-related equations may be as good or even better than the previous one (4.1). The Steinhart-Hart Equation (4.2) is commonly used when constructing circuits with an NTC 100K thermistor; thus, it is utilized in this thesis [42–45].

$$\frac{1}{T} = A + B\ln(R) + C\ln(R)^3 \tag{4.2}$$

T is the temperature in Kelvins, R the Resistance in ohms, and A, B and C Steinhart–Hart coefficients, which vary depending on the type and model of thermistor and the temperature range of interest.

The signal read by the arduino analogue input was the voltage at the point between the thermistor and a resistor connected to the ground, which as a value equivalent to the sensor (*e.g.* if it is an 10K NTC, it would be 10 KΩ). This value has a range between 0 and 1023, equivalent to 0V and 5V respectively. Using this information, we can know the resistor value of the thermistor by using equation 4.3, and thus applying it to the equation 4.2.

$$R_2 = R_1(\frac{V_{in}}{V_{out}} - 1) \tag{4.3}$$

R_1 and R_2 are the resistor values of the known thermistor resistors respectively, V_{in} 1023 (the 5V delivered from the arduino to the sensor), and V_{out} the value read in the analogue in pin.

A NTC 100K thermistor was chosen due to its better sensitivity and smaller size, allowing it better fit in the chamber and thus the R_1 is 100 kΩ.

4.2.2 Sensor calibration

When calibrating the sensors, it was necessary to consider two factors. The temperature relationship is influenced by both the volume of liquid inside the reaction tube and the precise positioning of the sensor. In relation to the first observation, in order to attain the same temperature in the liquid with varying quantities, there must be a increase in temperature detected by the sensor resulted by an increase of power delivered to the heating element. This phenomenon is evident when examining graphs A of Figures 3.5, 3.7 and 3.9, which depict the temperature values required in the heating element to attain an internal temperature of 65°C. The values of temperature are 78°C, 72.5°C, and 66°C, respectively. This phenomenon is also evident in the software SimScale, as depicted in Figure A.3.

Before building the box, with the setup mentioned in chapter 2 subsection 2.2.2, the values obtained from the sensor can be influenced to a certain extent by its position, as demonstrated in the SimScale Figures (*e.g.*, Figure 3.2). By comparing graphs B of Figures 3.6 with 3.7 and 3.8 alongside 3.9, it can be inferred that the sensor located in chamber 2 exhibits a slightly shorter distance to the heating element. Consequently, the temperature

experienced by this sensor rises at a faster rate compared to the temperature inside the reaction tube. Given that the block is composed of aluminum and its position may vary by a few millimeters, there was no necessity to attempt repositioning, as ultimately the desired temperature was still attained.

In order to display the temperature information to the user, a proportional relationship was established between the maximum temperatures of the block and the reaction tube. This ratio was then applied to the sensor values for temperature measurement. Due to the inability of the thermometer to make contact with the small volume of liquid in the LAMP assay, the temperatures corresponding to this assay could not be measured. As a result, an average value was calculated by taking the midpoint between the ratios obtained from a liquid volume of 0.1 mL (0.725) and 0.0 mL (0.978) (Figures 3.6 and 3.8 respectively) . The final calculated ratio was 0.936, due to the low volume of the assay.

After building the box and placing all the components inside it, the calibration was made again since there could be some displacement of either the heating elements or the sensors. Also the chambers are now more isolated, with an addition of the walls of the box and one layer of polyethylene isolation material (described in chapter 2 subsection 2.2.2). This time the calibration was made with a liquid volume of 40 μL, since at this time a solution was found to get the NTC 100k thermistor working under water, by embedding it in epoxy to make it impermeable. In order to make this acquisition more automate, a python code was made that recorded the values of the sensors every 10 seconds, while saving them in a txt file (link to the code in appendix A).

Figures 3.10 and 3.11 indicate that the target temperatures were achieved, but there was a notable delay between the temperature inside the reaction tube and the temperature in the chamber hole, particularly in chamber 2. The observed delay in the second chamber may possibly be also attributed to the absence of epoxy application for shaping a reaction tube format, which would serve as proof its efficiency. To provide an approximate temperature reading to the user, rather than directly using the equations derived from Figures 3.10B and 3.11B, a ratio was calculated between the temperature measured in the chamber hole when it reached 65.5°C and the desired working temperature. This ratio was applied to both chambers. In chamber 1 the value is of 0.96 and in chamber 2 is 0.95. This values indicate that a better isolation was obtained when compared with the estimated value of 0.936.

Comparing Figure 2.1 A) and B), we conclude that with the NTC sensor, the results were more accurate since the sensor tip was fully immersed in the liquid, while the thermometer sensor was not, and so the temperature read by it could also be of the air inside the tube.

4.2.2.1 Heating time

Since temperature readings before device assembly were obtained by placing an NTC 100k thermistor in a hole drilled into the aluminum of the chamber, an additional 3 minutes

are added to the waiting period recorded with 1 mL of liquid volume (which was 7.5 minutes) to enable the heat to ensure the temperature was evenly distributed throughout the chamber, ending with approximately a 10 minute time.

Upon completion of the device assembly, the duration required for heating was seen to be reduce to around 3.5 to 4 minutes, resulting in a total heating time of 7 minutes with the additional time. This occurrence can be attributed to the presence of an extra layer of isolation and the enclosure of the chambers from the external environment.

4.2.3 Power consumption

One of the most crucial steps to do when building a portable device is to make sure that it can be used several times in one charge. In order to ascertain the appropriate capacity of a power bank, tests are conducted to evaluate power consumption.

In order to compute the power bank duration for all potential scenarios, namely the absence, presence, or dual activation of chambers, current measurements were obtained for each respective condition. The endurance of the device was determined by multiplying the capacity of the power bank by the current measured. With a storage capacity of 20,000 mAh, the device would be capable of sustaining operation for an estimated duration of 247 hours in idle mode. When one chamber was activated, the device can operate for approximately 25 hours, and when both chambers are activated, the operational time reduces to approximately 14 hours. Assuming that 100 % of the total duration of the 30-minute assay was occupied by the activation of the heating elements. The inclusion of the initial 7-minute heating period, starting from ambient temperature and reaching 65 °C, leads to a cumulative power consumption of 37 minutes. Given the aforementioned factors, the device will function for a duration of 14 hours or a minimum of 22 tests.

In order to verify the accuracy of these calculations, a series of consecutive 30-minute assessments were conducted utilizing both heating chambers. These assessments were followed by 10-minute breaks. It was observed that the 20000 mAh power banks were only able to sustain 10 assessments before depleting their charge. This phenomenon may be attributed to either a potential flaw in the power bank or a potential power consumption resulting from communication between the microcontroller and the battery. To refute this theory, an experiment was conducted with an additional 10000 mAh power bank, where no breaks where made. The power supply once again exhibited a duration that was barely half of the anticipated period, of 3.5 hours.

Upon conducting code revisions, it was discovered that the specific segment of code responsible for altering the voltage from 5 V to 12 V consistently remained active, resulting in continuous energy use. By modifying the code to restrict communication inside the initial 5-second timeframe upon device activation, and afterwards conducting the assay again using the 10 Ah power bank, the duration from complete charge to complete discharge was seen to be 6.5 hours. This span was just 0.5 hours shorter than the expected duration. Based on extrapolation, it may be inferred that the 20 Ah battery would have a

duration of around 13 hours.

4.3 Box construction

The decision to employ 3D printing as the manufacturing method for the device's box case was driven by its capacity to accelerate the production and assembly of materials. This choice streamlines rapid prototyping and permits swift adjustments if needed. Notably, the company responsible for producing the parts completed the task in just two weeks, at a cost of 95€.

The box was designed to have enough space to fit all the electronic components inside, as well as having openings to place all the components supposed to be visible by the user, such as the screen and buttons. Also an thickness of 4 mm for each part was selected in order to avoid collapsing of the structure during travels.

During the LAMP tests, no damage was observed in the device due to elevated temperatures.

4.4 Filtration

The utilization of a filtration system to capture pathogens is a widely adopted procedure owing to its straightforwardness, which involves the passage of a liquid containing the sample through the membrane filter. One crucial factor to consider is the pore size, as it must be sufficiently small to impede the passage of the target pathogen, while still allowing the passage of other substances. The selection of a 0.45 μm PVDF filter membrane (Durapore®) was based on the sizes of *E.coli* and *E.faecalis*, averaging 1μm [46].

The experiment exhibited the ability of the designed structure to securely retain the filter, preventing any slippage, while also providing sufficient openings for the passage of liquid without causing damage to either the base or the filter. This outcome serves as evidence that the iglidur® i8-ESD material (Cologne, Germany) is appropriate for such assays, as anticipated based on the examination of the datasheet (data now shown).

The primary objective of the pre-filter phase was to prevent the unnecessary entrapment of components in the filter, which could result in partial or complete blockage. This would prolong the filtration process or potentially render it impossible. Table 3.1 illustrates a positive correlation between the number of assays and the corresponding increase in time. Furthermore, in order to mitigate the extended duration, additional force was exerted on the syringe subsequent to doing 20 trials.

Ideally, the pre-filter should be replaced after each use. However, in situations where there is a scarcity, it may be utilized up to approximately 20 times, provided that the assays yield negative results and the local area being tested is the same. After conducting 20 tests, the system started encountering obstructions, requiring an increase in the applied force to allow water to flow through. This is evident in Figure 3.14, which shows a gradual increase in the yellow hue after every 10 tests. Consequently, the pre-filter would begin

to exhibit remnants of the pathogens of interest, so contaminating subsequent samples. These results were observed using seawater from Carcavelos Beach, collected at 10:00 AM. The water was found to be free of algae and contained minimal dirt.

To facilitate the passage of target pathogens, the pre-filter pore size should be higher than 1 micrometer. Since the pre-filter used in out test is the CHROMAFIL® Xtra PET, 25 mm, 1 µm (Nordrhein-Westfalen, Germany); there is a possibility to lose some of our interest bacteria because the with of an *E.coli* is around 1 μm and the *E.faecalis* 0.5 μm to 1 μm. In future tests it would be necessary to buy a pre-filter with a larger pore size (*e.g.* CHROMAFIL® Xtra PET, 25 mm, 1.2 µm (Nordrhein-Westfalen, Germany) or CHROMAFIL® Xtra PES, 25 mm, 5 µm (Nordrhein-Westfalen, Germany)).

4.5 LAMP assays

After performing a LAMP assay with the device, the detection process yields a binary outcome, indicated by a color transition in the membrane on top of the reaction tube from yellow (representing negative) to pink (representing positive). The assay was conducted under controlled laboratory conditions, thereby reducing the risks associated with contamination by environmental factors, where one assay was conducted for each pathogen.

Figure 3.15 depicts the assays made with *Enterococcus faecalis*, where it was observed a reaction devoid of any contamination in the reaction tubes situated within both the device and the thermocycler. The positive tube in the thermocycler exhibited a more rapid reaction and greater intensity of color than in the portable device. This phenomenon may be attributed to the displacement of the Grade 4 Paper Whatman®, which enables the liquid get in contact with both sides of the paper, resulting in an enhanced color change reaction. This displacement can be seen in figure 3.15, where the paper is not totally fixed in the cap. Figure A.8 illustrate the comparison of the tubes utilized in the device, highlighting the enhanced visibility of color differentiation within them.

Figure A.7 depicts the identical content as Figure 3.15, albeit with the inclusion of *Escherichia coli* as the pathogenic organism. Even though there were no dislocations in the current experiment, and the results obtained from both the device and the thermocycler closely resembled each other, some contamination is still possible to observe. This is evident as each pair of reaction tubes displayed a positive color, which became more noticeable at the 20-minute mark. To validate these findings, another assay with E. coli was conducted, where no contamination was observed (as shown in Figure 3.16). The variation rate of color change remained observable, indicating that the displacement of the Grade 4 Whatman® paper was not the cause of this phenomenon.

This variation could be attributed to temperature discrepancies, wherein the device does not have the same calibration as the thermocycler's temperature. In this particular instance, it is advisable to conduct measurements by inserting a sensor into the thermocycler to ensure the precision of temperature readings. This discrepancy arises because

the temperature displayed on the thermocycler could corresponds to the heating element, while our prototype has been specifically calibrated to measure the temperature inside the reaction tube.

When we measured the actual temperature inside a reaction tube with 40 μL of liquid in the thermocycler, we noticed a discrepancy. Even though the display showed 65°C, the NTC 100K sensor registered a temperature of 69.5°C. Furthermore, by referring to Figure A.3 in Appendix A, we can conclude that the calibration of the thermocycler was done by using a tube filled to its full liquid capacity. This is because when there's more liquid in the tube, the heating element needs to reach a higher temperature to achieve the target temperature inside. Since the thermocycler presents better results, recalibration of the portable device to 69.5°C needs to be done.

Given that the intensity of color in the positive tubes remained stable even after 15 to 20 minutes, the results offer strong evidence of the device's ability to maintain temperature effectively. This enables the successful execution of LAMP assays within it, albeit with a slight delay in the color change compared to when the thermocycler is employed.

When determining the cost per test, it was found that the device components have an estimated cost of around 150€, the box costs 95€ (resulting in 245 € total), and the reagent required for the LAMP assay has a cost of 1€ or less. The estimated lifespan of the device is three years, with each year consisting of 52 weeks. Assuming a minimum of four assays are conducted each week, this results in around 624 assays per year. Consequently, the cost per assay may be calculated by adding the costs of the LAMP reagents to the result of the division of 240 by 624, or 1.40€ per assay. When production occurs within an industry, the price tends to decrease as a result of material discounts stemming from larger purchases. Consequently, the cost per test can be further reduced.

5

Conclusion

The data acquired through the conducted simulations facilitated the selection of the most optimal model among the various options presented. Additionally, it provided guidance on the appropriate placement of the sensors and offered valuable insights into the significance of accurately determining the appropriate amount of power to the heating element, whether through a 12 V power bank or a power socket. This information helped to reach a peak result of having a 7 minute heating time, with 3 extra minutes included. Additionally, by utilizing optimal energy consumption, the power bank was able to sustain a minimum duration of 13 hours.

Simulations of the circuit served as a valuable tool for identifying potential issues, selecting appropriate components, and initiating the final code. This code successfully facilitated the reading of temperature sensors, enabling the adjustment of power supplied to the heating element. Additionally, it accurately displayed relevant information for both chambers on the screen. The system also allowed users to customize the duration of the assay using either a rotary encoder or two separate buttons. Furthermore, it provided functionality to start and pause the assay, while appropriately illuminating LEDs to indicate the current state of the process (red for heating, green for readiness, and blue for completion). Auditory signals were incorporated to accompany these visual cues, and a reset button was included to rectify any inadvertent assay initiation. The construction of the box was highly customized thanks to 3D printing technology, which allowed to fit all the components inside it, while having the structural integrity needed to support the components. The filtration system was also constructed using the same technology, therefore enabling adaptation to an existing system by simply replacing a single component.

Ultimately, the LAMP assays have proven successful, thereby validating the culmination of earlier experiments and resulting in the development of a portable device with the ability to conduct assays, either on pathogens related recreational waters, or human connected ones (*e.g , Candida*). As future perspectives, the device and the filtration system should be tested alongside the entity responsible to perform these tests in recreational waters.

Bibliography

[1] J. M. Lourenço. *The NOVAthesis LaTeX Template User's Manual*. NOVA University Lisbon. 2021. URL: https://github.com/joaomlourenco/novathesis/raw/main/template.pdf.

[2] L. Fogarty et al. "Abundance and characteristics of the recreational water quality indicator bacteria escherichia coli and enterococci in gull faeces". In: *Journal of Applied Microbiology* 94.5 (2003), pp. 865–878. DOI: 10.1046/j.1365-2672.2003.01910.x.

[3] T. Hänscheid and M. P. Grobusch. "How useful is PCR in the diagnosis of malaria?" In: *Trends in Parasitology* 18.9 (2002), pp. 395–398. DOI: 10.1016/s1471-4922(02)02348-6.

[4] I. R. Poxton. "Molecular techniques in the diagnosis and management of infectious diseases: Do they have a role in bacteriology?" In: *Medical Principles and Practice* 14.Suppl. 1 (2005), pp. 20–26. DOI: 10.1159/000086181.

[5] G. L. Gilbert. "Molecular diagnostics in infectious diseases and public health microbiology: Cottage industry to postgenomics". In: *Trends in Molecular Medicine* 8.6 (2002), pp. 280–287. DOI: 10.1016/s1471-4914(02)02349-3.

[6] F. Ramírez-Castillo et al. "Waterborne pathogens: Detection methods and challenges". In: *Pathogens* 4.2 (2015), pp. 307–334. DOI: 10.3390/pathogens4020307.

[7] T. Notomi. "Loop-mediated isothermal amplification of DNA". In: *Nucleic Acids Research* 28.12 (2000). DOI: 10.1093/nar/28.12.e63.

[8] M. Karamanou et al. "Anton van Leeuwenhoek (1632-1723): Father of micromorphology and discoverer of spermatozoa". In: *Revista Argentina de microbiología* 42 (2010), pp. 311–4. DOI: 10.1590/S0325-75412010000400013.

[9] S. M. Blevins and M. S. Bronze. "Robert Koch and the 'Golden Age' of bacteriology". In: *International Journal of Infectious Diseases* 14.9 (2010). DOI: 10.1016/j.ijid.2009.12.003.

[10] E. Genome. *steps*. URL: https://loopamp.eiken.co.jp/en/lamp/0211.html.

[11] E. Genome. *Animation*. URL: https://loopamp.eiken.co.jp/en/lamp/0203.html.

[12] N. Tomita et al. "Loop-mediated isothermal amplification (LAMP) of gene sequences and simple visual detection of products". In: *Nature Protocols* 3.5 (2008), pp. 877–882. DOI: 10.1038/nprot.2008.57.

[13] W.-F. Du et al. "Single-step, high-specificity detection of single nucleotide mutation by primer-activatable loop-mediated isothermal amplification (PA-lamp)". In: *Analytica Chimica Acta* 1050 (2019), pp. 132–138. DOI: 10.1016/j.aca.2018.10.068.

[14] Y. Mori and T. Notomi. "Loop-mediated isothermal amplification (LAMP): A rapid, accurate, and cost-effective diagnostic method for infectious diseases". In: *Journal of Infection and Chemotherapy* 15.2 (2009), pp. 62–69. DOI: 10.1007/s10156-009-0669-9.

[15] H. Kaneko et al. "Tolerance of loop-mediated isothermal amplification to a culture medium and biological substances". In: *Journal of Biochemical and Biophysical Methods* 70.3 (2007), pp. 499–501. DOI: 10.1016/j.jbbm.2006.08.008.

[16] M. Seki et al. "Loop-mediated isothermal amplification methods for diagnosis of bacterial meningitis". In: *Frontiers in Pediatrics* 6 (2018). DOI: 10.3389/fped.2018.00057.

[17] K. Nagamine, T. Hase, and T. Notomi. "Accelerated reaction by loop-mediated isothermal amplification using loop primers". In: *Molecular and Cellular Probes* 16.3 (2002), pp. 223–229. DOI: 10.1006/mcpr.2002.0415.

[18] Y. Mori et al. "Real-time turbidimetry of lamp reaction for quantifying template DNA". In: *Journal of Biochemical and Biophysical Methods* 59.2 (2004), pp. 145–157. DOI: 10.1016/j.jbbm.2003.12.005.

[19] T. Notomi. *LAMP primer designing software*. 2000. URL: http://primerexplorer.jp/e/.

[20] S. Lukinmaa et al. "Application of molecular genetic methods in diagnostics and epidemiology of food-borne bacterial pathogens". In: *APMIS* 112.11-12 (2004), pp. 908–929. DOI: 10.1111/j.1600-0463.2004.apm11211-1213.x.

[21] S. Fallahi et al. "Diagnosis of *Candida albicans*: Conventional diagnostic methods compared to the loop-mediated isothermal amplification (LAMP) assay". In: *Archives of Microbiology* 202.2 (2019), pp. 275–282. DOI: 10.1007/s00203-019-01736-7.

[22] S. J. Silva, K. Pardee, and L. Pena. "Loop-mediated isothermal amplification (LAMP) for the diagnosis of zika virus: A Review". In: *Viruses* 12.1 (2019), p. 19. DOI: 10.3390/v12010019.

[23] P. S. Bhavan et al. "Culture and identification of candida albicans from vaginal ulcer and separation of enolase on SDS-PAGE". In: *International Journal of Biology* 2.1 (2010). DOI: 10.5539/ijb.v2n1p84.

[24] M. Ito et al. "Rapid detection and typing of influenza A and B by loop-mediated isothermal amplification: Comparison with immunochromatography and virus isolation". In: *Journal of Virological Methods* 135.2 (2006), pp. 272–275. DOI: 10.1016/j.jviromet.2006.03.003.

[25] M. Imai et al. "Development of H5-RT-lamp (loop-mediated isothermal amplification) system for rapid diagnosis of H5 avian influenza virus infection". In: *Vaccine* 24.44-46 (2006), pp. 6679–6682. DOI: 10.1016/j.vaccine.2006.05.046.

[26] C. Amaral et al. "A molecular test based on RT-lamp for rapid, sensitive and inexpensive colorimetric detection of SARS-COV-2 in clinical samples". In: *Scientific Reports* 11.1 (2021). DOI: 10.1038/s41598-021-95799-6.

[27] S.-C. Sheu, Y.-S. Song, and J.-J. Chen. "A portable continuous-flow polymerase chain reaction chip device integrated with Arduino boards for detecting Colla Corii Asini". In: *Micromachines* 13.8 (2022), p. 1289. DOI: 10.3390/mi13081289.

[28] S. Di Nonno and R. Ulber. "Portuino—a novel portable low-cost Arduino-based photo- and fluorimeter". In: *Sensors* 22.20 (2022), p. 7916. DOI: 10.3390/s22207916.

[29] A. H. Velders, C. Schoen, and V. Saggiomo. "Loop-mediated isothermal amplification (LAMP) shield for Arduino DNA detection". In: *BMC Research Notes* 11.1 (2018). DOI: 10.1186/s13104-018-3197-9.

[30] K. R. Sreejith et al. "A portable device for lamp based detection of SARS-COV-2". In: *Micromachines* 12.10 (2021), p. 1151. DOI: 10.3390/mi12101151.

[31] S. Lee et al. "Rapid and in-situ detection of fecal indicator bacteria in water using simple DNA extraction and portable loop-mediated isothermal amplification (LAMP) PCR methods". In: *Water Research* 160 (2019), pp. 371–379. DOI: 10.1016/j.watres.2019.05.049.

[32] G. Papadakis et al. "Portable real-time colorimetric lamp-device for rapid quantitative detection of nucleic acids in crude samples". In: *Scientific Reports* 12.1 (2022). DOI: 10.1038/s41598-022-06632-7.

[33] A. B. Zia et al. "Development of microfluidic lab-on-disc based portable blood testing point-of-care diagnostic device". In: *2016 IEEE EMBS Conference on Biomedical Engineering and Sciences (IECBES)*. 2016, pp. 142–145. DOI: 10.1109/IECBES.2016.7843431.

[34] J. N. Reddy. *An introduction to the finite element method*. McGraw-Hill, 2006.

[35] L. D. L. *A first course in the finite element method*. Cengage Learning, 2011.

[36] N. Divya et al. "Design and Implemetation of Combinational Logic Circuits using Open Source Tool". In: *2022 International Conference on Automation, Computing and Renewable Systems (ICACRS)* (2022). DOI: 10.1109/icacrs55517.2022.10029180.

[37] R. Martzy et al. "A loop-mediated isothermal amplification (LAMP) assay for the rapid detection of enterococcus spp. in water". In: *Water Research* 122 (2017), pp. 62–69. DOI: 10.1016/j.watres.2017.05.023.

[38] Y. Guo et al. "Factors affecting thermal conductivities of the polymers and polymer composites: A review". In: *Composites Science and Technology* 193 (2020), p. 108134. DOI: 10.1016/j.compscitech.2020.108134.

[39] W. Yu. "Simulation and Experimental Study of Temprature Lag Time for Polymerase Chain Reaction Instrument". In: *BMEI 2010: Proceedings, 2010 3rd International Conference on Biomedical Engineering and Informatics: 16-18 October 2010, Yantai, China*. IEEE, 2010, pp. 1591–1594.

[40] J. Carvill. "Thermodynamics and heat transfer". In: *Mechanical Engineer's Data Handbook* (1993), pp. 102–145. DOI: 10.1016/b978-0-08-051135-1.50008-x.

[41] J. D. Bronzino. *Medical Devices and Systems*. CRC/Taylor amp; Francis, 2006.

[42] Circuitgeeks. *Make an Arduino temperature sensor using thermistor*. 2022. URL: https://www.circuitgeeks.com/arduino-temperature-sensor-thermistor/.

[43] S. Campbell. *Make an Arduino temperature sensor (thermistor tutorial)*. 2023. URL: https://www.circuitbasics.com/arduino-thermistor-temperature-sensor-tutorial/.

[44] A. Brandis et al. "Temperature control concept for parallel IGBT operation". In: *Electronics* 10.4 (2021), p. 429. DOI: 10.3390/electronics10040429.

[45] M. Petkovšek, M. Nemec, and P. Zajec. "Algorithm execution time and accuracy of NTC thermistor-based temperature measurements in time-critical applications". In: *Mathematics* 9.18 (2021), p. 2266. DOI: 10.3390/math9182266.

[46] Z. Kotsiri and A. Vantarakis. "Evaluation of seawater monitoring for the detection of escherichia coli and enterococcus faecalis on an integrated biosensor system". In: *Sensor Review* 43.2 (2023), pp. 92–98. DOI: 10.1108/sr-09-2022-0380.

A

Appendix

GitHub repository: `https://github.com/INeca13/thesis`.

Tinkercad provisional code: `https://github.com/INeca13/thesis/blob/main/tinkercad_program.ino`.

Final code: `https://github.com/INeca13/thesis/blob/main/timer_two_chambers_65_12V_5V_testes0_8_1.ino`.

Sensor recording code: `https://github.com/INeca13/thesis/blob/main/sensor%20values%20recording.py`

Box 3D models: `https://github.com/INeca13/thesis/tree/main/3D%20Models/Box`

3D Filter model: `https://github.com/INeca13/thesis/tree/main/3D%20Models/Filter`

3D Heat Models: `https://github.com/INeca13/thesis/tree/main/3D%20Models/Heat%20models`

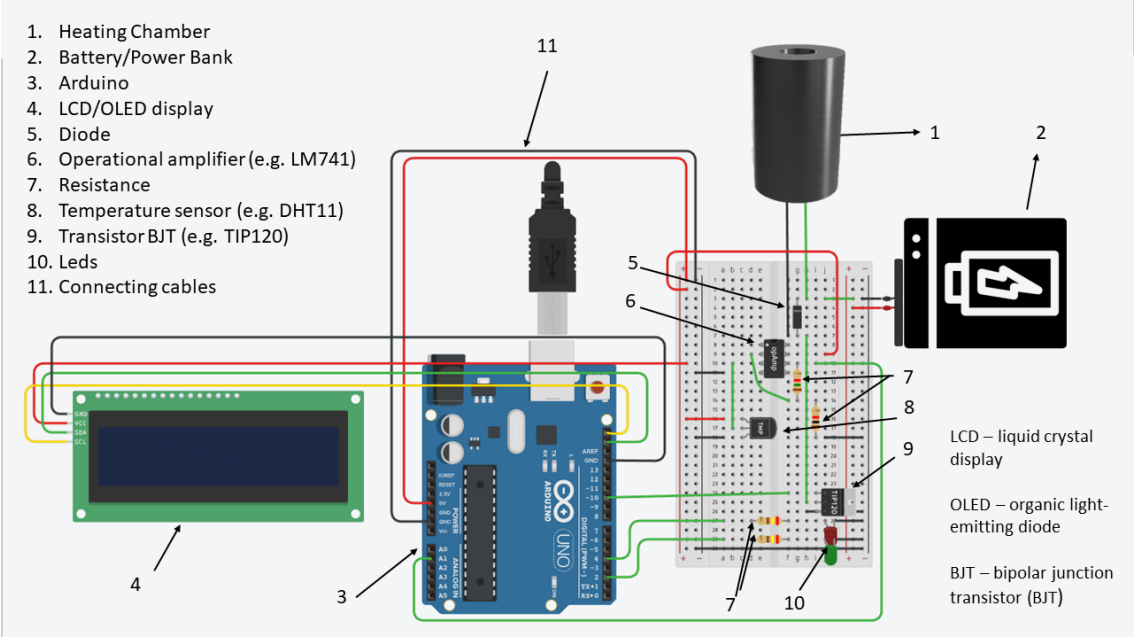

Figure A.1: Ilustration of the circuit simulated in Tinkercad

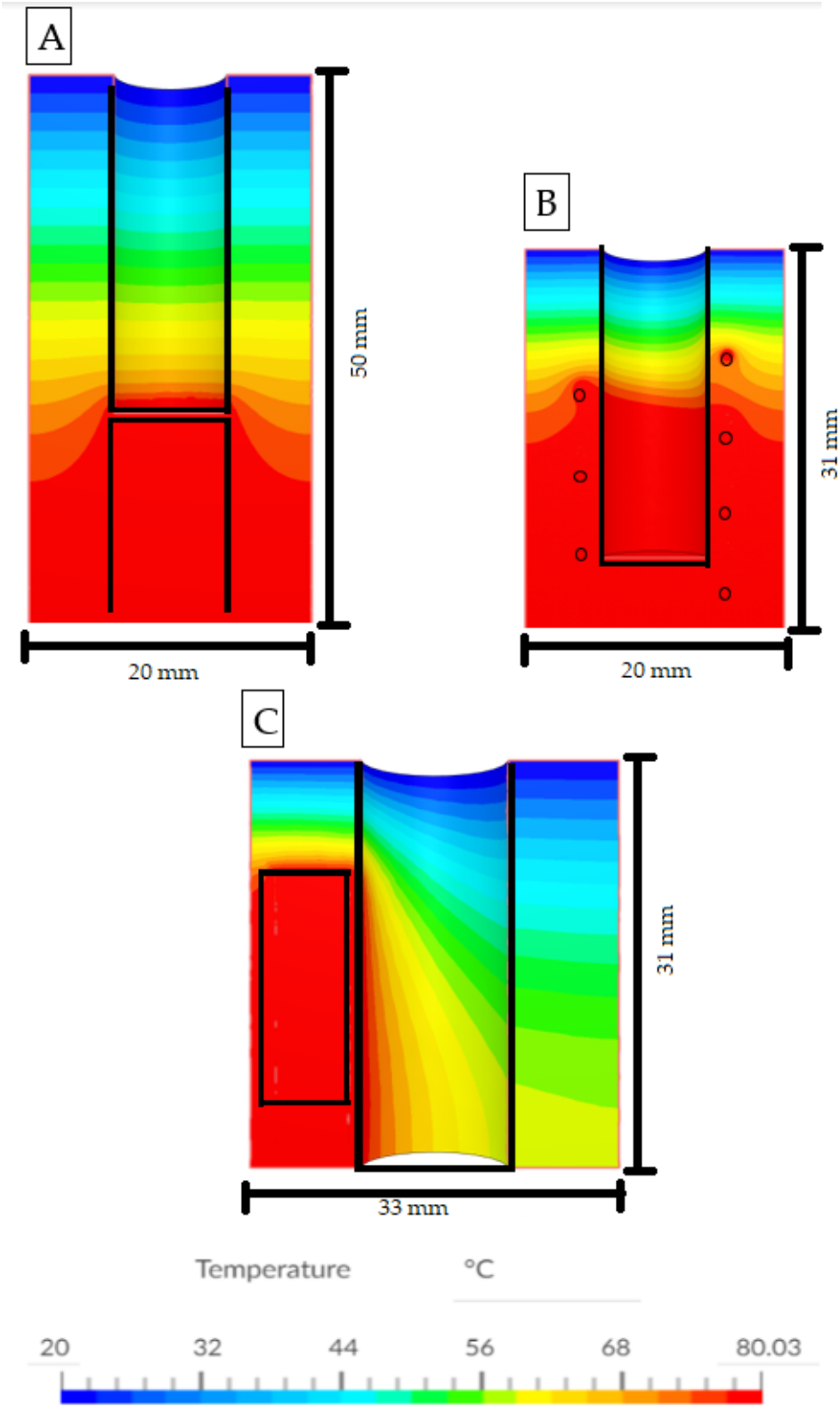

Figure A.2: Simulation of the chamber temperature A) with Cartridge heating configuration, B) with a nichrome wire heating configuration and with C) Cartridge heating from the side configuration

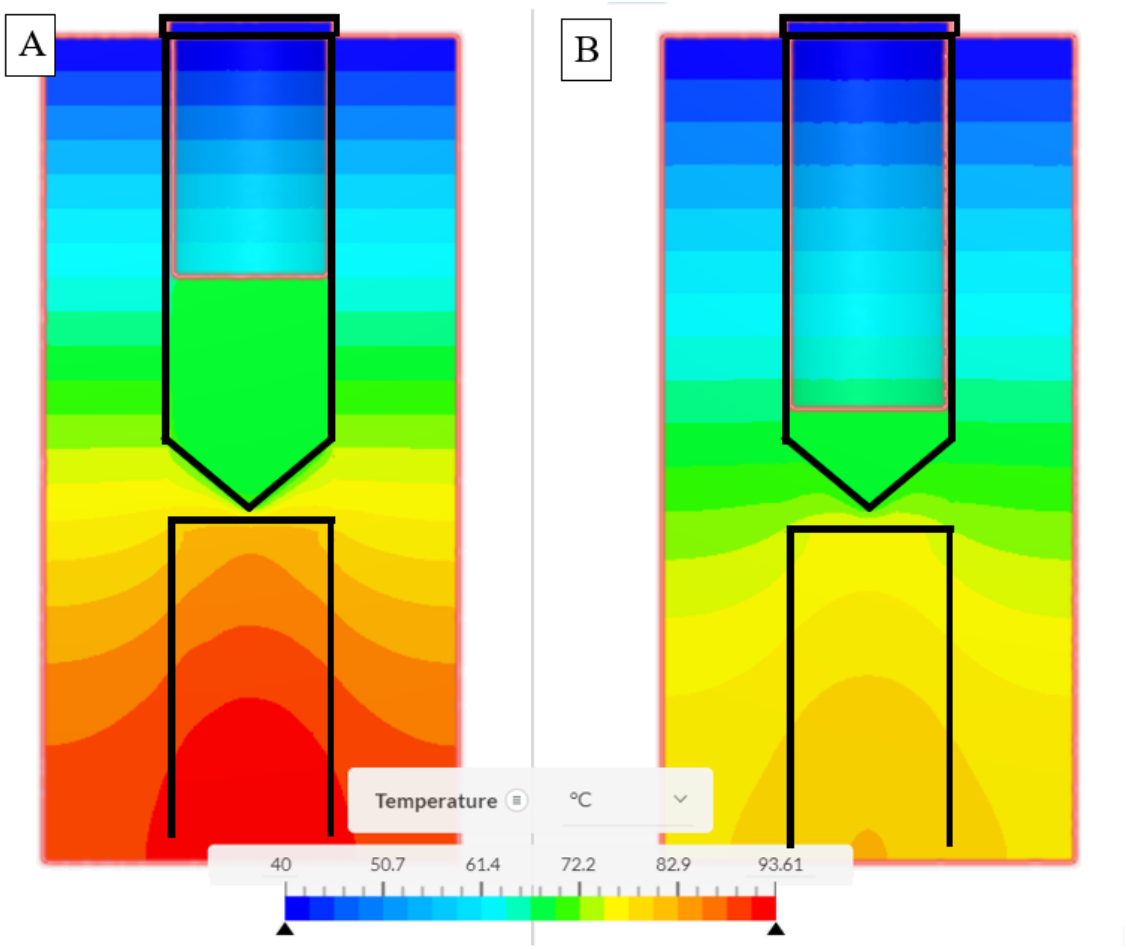

Figure A.3: A) LAMP temperature with half full and B) real liquid volume in the reaction tube

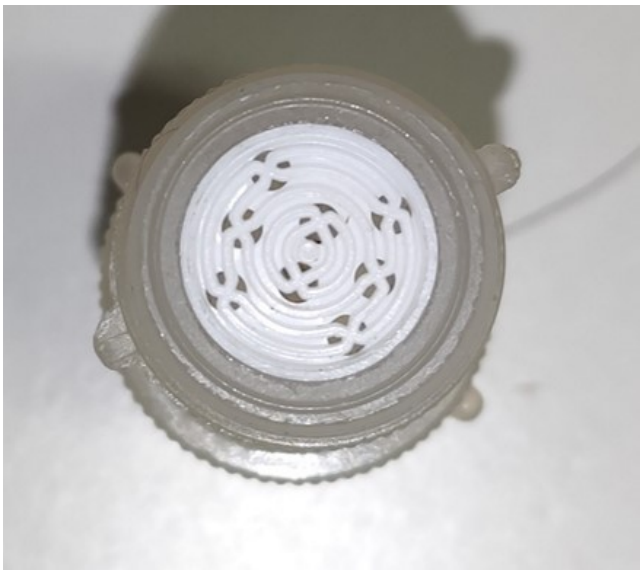

Figure A.4: Filter before adaptation, where the filters used measure 10 mm of diameter

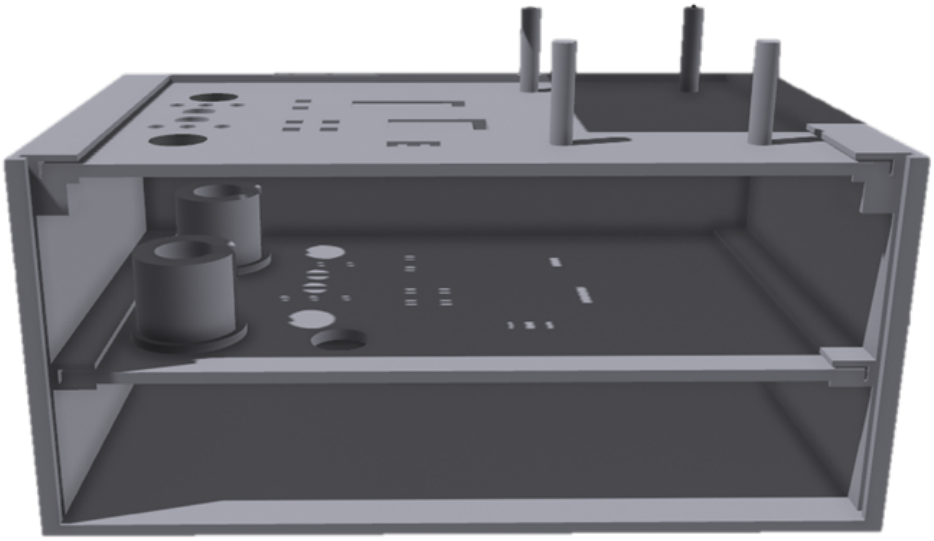

Figure A.5: Sketch of the device done Shapr3D software

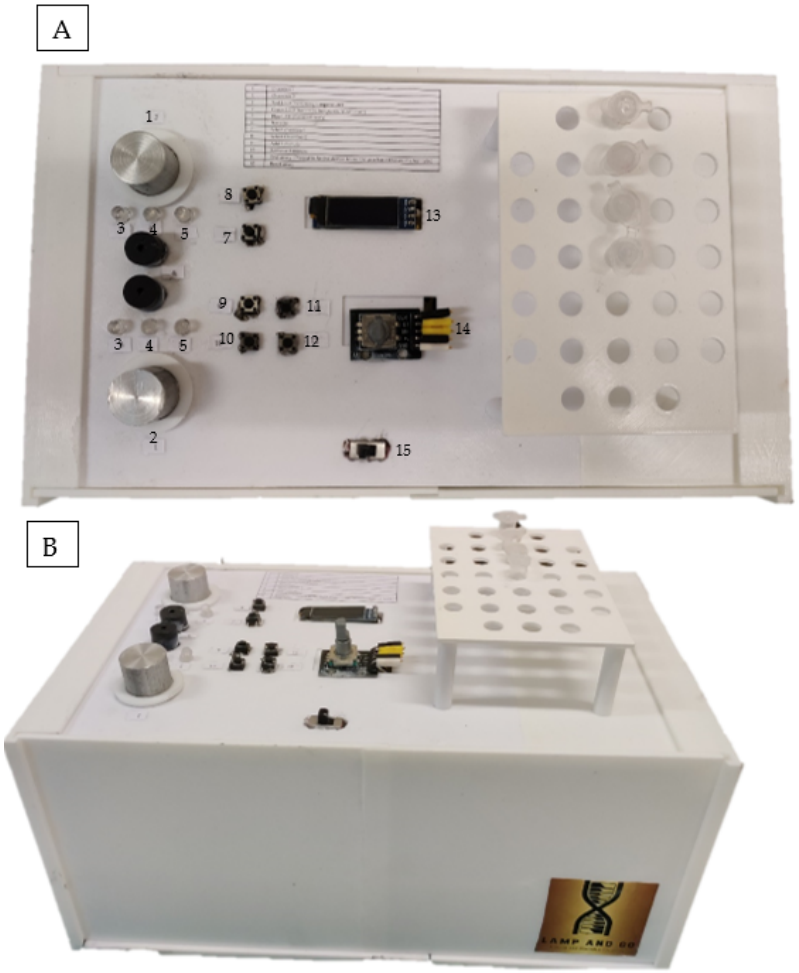

1	Chamber 1
2	Chamber 2
3	Red LED (increasing temperature)
4	Green LED (favorable temperature achieved)
5	Blue LED (Finished assay)
6	Buzzers
7	Select chamber 1
8	Select Chamber 2
9	Add 1 minute
10	Remove 1 minute
11	End assay (Pressed to let the device know the user has retrieved the test tube)
12	Reset assay
13	OLED Screen
14	Rotary encoder
15	On/Off Switch

Figure A.6: Final build of the device, A) represents all the components visible to the user, with the respective labelling, B) is a general view of the box, also showing the logo made for the prototype

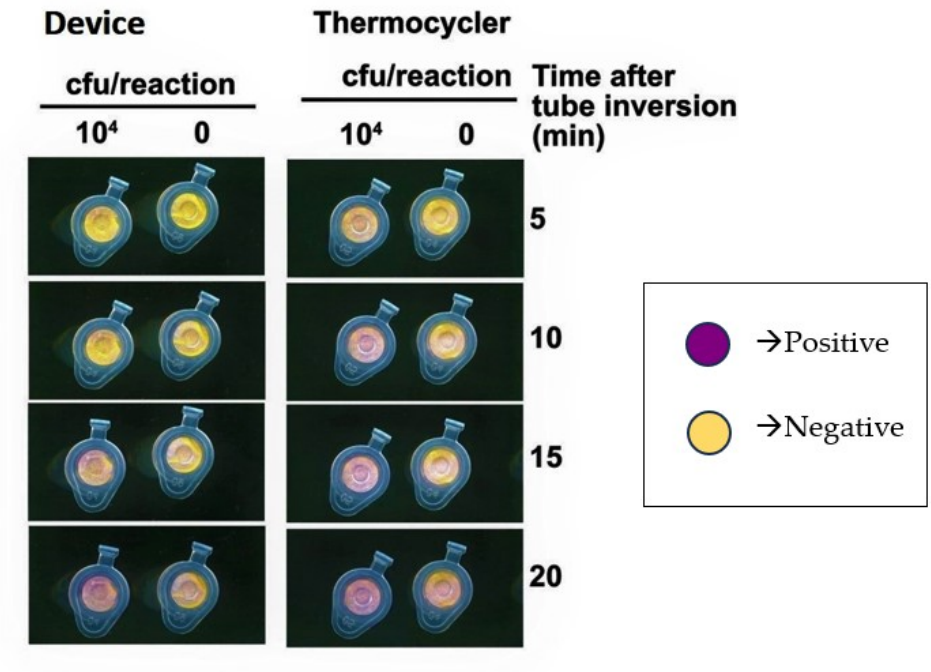

Figure A.7: LAMP assay of *Escherichia coli* in the portable device and the thermocycler

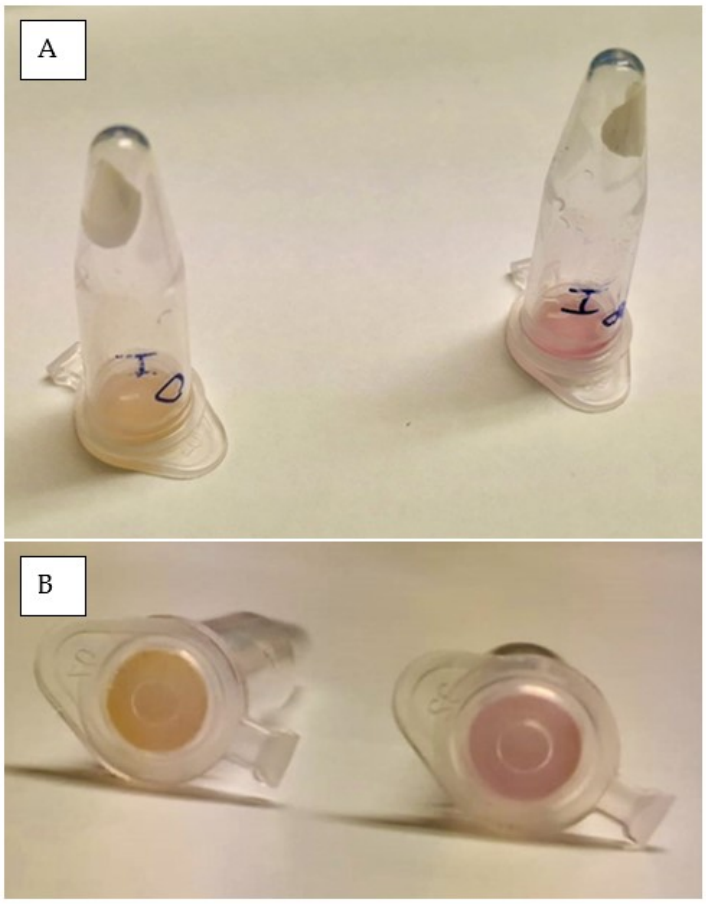

Figure A.8: Picture of control vs *E.faecalis* presence, depicting the visual difference noted when observing A) the inner part of the membrane and in B) the cap of the tube

Figure A.9: Picture of *Candida albicans* presence vs control in the device (first two tubes of the left) and in the thermocycler (last two), depicting the visual difference noted when observing A) the cap of the tube and in B) the inner part of the membrane

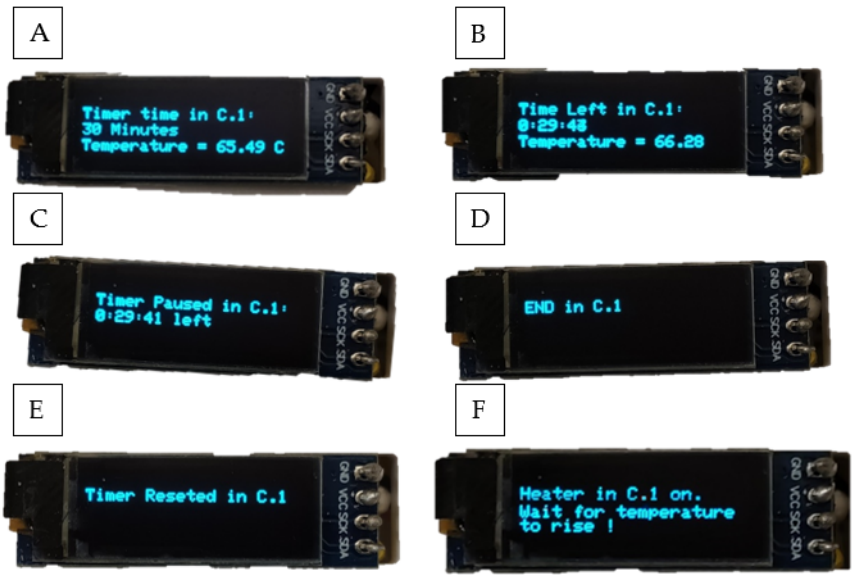

Figure A.10: Possible menus displayed to the user in one chamber where A) presents the current temperature as well as the time programmed to the assay, B) the timer in countdown with the assay running and also the temperature, C) the information of the assay being paused and the time left to end, D) the end of an assay in the chamber, E) the resetting screen and F) when the user turns on the heating element and/or when wants to start an assay and the temperature is not adequate.